PERIMETER INSTITUTE FOR THEORETICAL PHYSICS

Modified Gravity (MOG), Dark Matter and Black Holes

John Moffat

Perimeter Institute

Miami 2015 Conference

Fort Lauderdale, December 16, 2015


THE DARK MATTER - DARK ENERGY
CONUNDRUM
deskarati.com

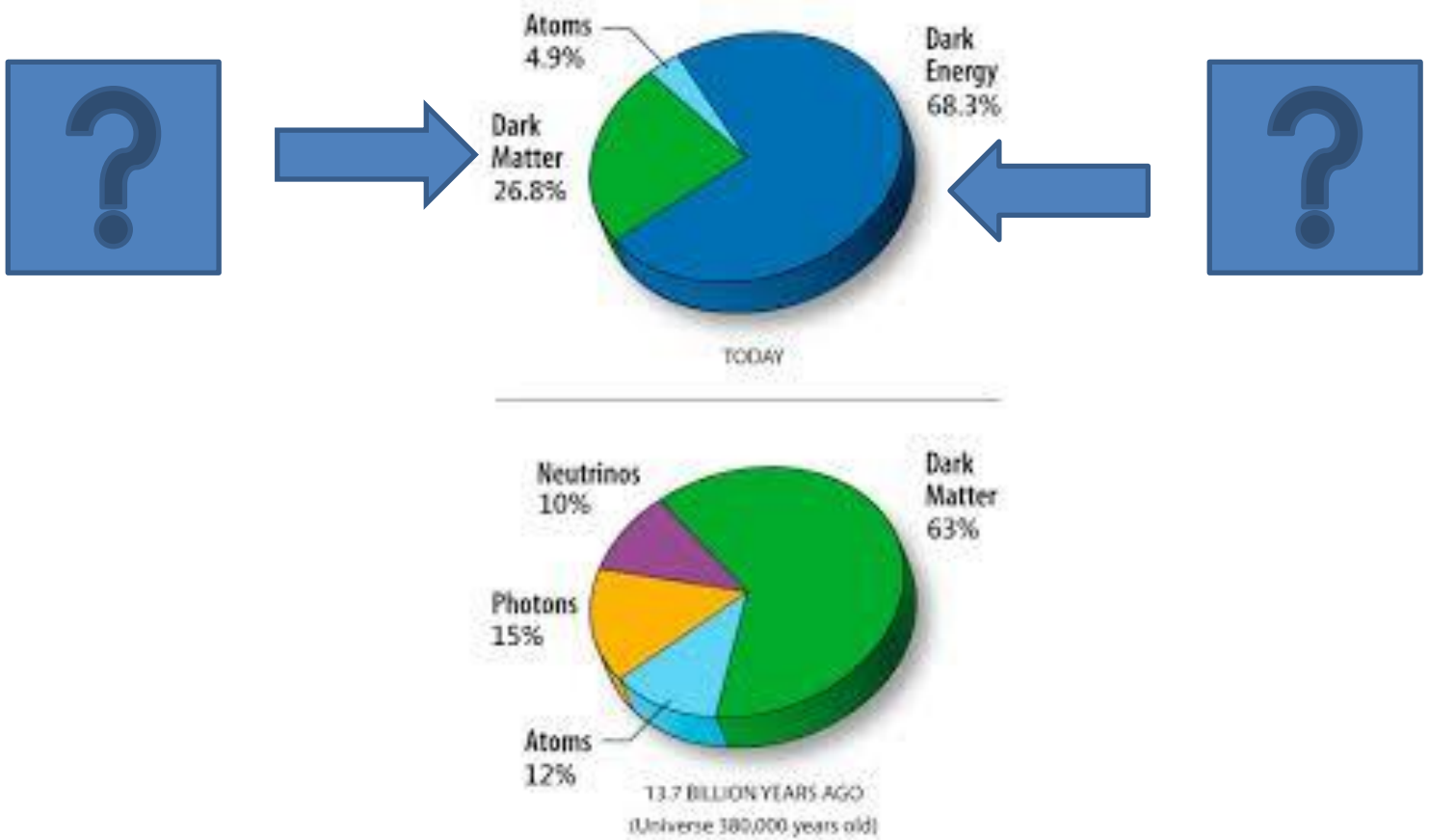
Atoms
4.9%
Dark
Matter
26.8%
Dark
Energy
68.3%
TODAY
Neutrinos
10%
Photons
15%
Atoms
12%
Dark
Matter
63%
13.7 BILLION YEARS AGO
(Universe 380,000 years old)

https://angel.co/mog

Introduction

- Observations of the dynamics of galaxies as well as the dynamics of the whole Universe reveal that a main part of the Universe's mass must be missing or, in modern terminology, this missing mass is made of dark matter. The universe is observed to undergo an accelerated expansion (dark energy).

- Observations of galaxies reveal that there is a discrepancy between the observed dynamics and the mass inferred from luminous matter (Rubin et al. 1965, Rubin & Ford 1970).

- An alternative approach to the problem of missing mass is to replace dark matter by a modified gravity theory. The generally covariant Modified Gravity (MOG) theory is a scalar-tensor-vector theory (STVG, JM, JCAP, 0603 004 (2006), arXiv:0506021 [gr-qc]).

- The LUX experimental data from the Sanford Underground Research Facility (Lead, South Dakota) using a 370 kg liquid Xenon detector has ruled out low-mass WIMPs, and set new bounds on elastic scattering cross sections of WIMPs. No WIMP signals were detected. To-date no convincing detection of dark matter particles has been achieved in either laboratory or satellite experiments.

D. S. Akerib et al. (LUX Collaboration), arXiv:1512.03506

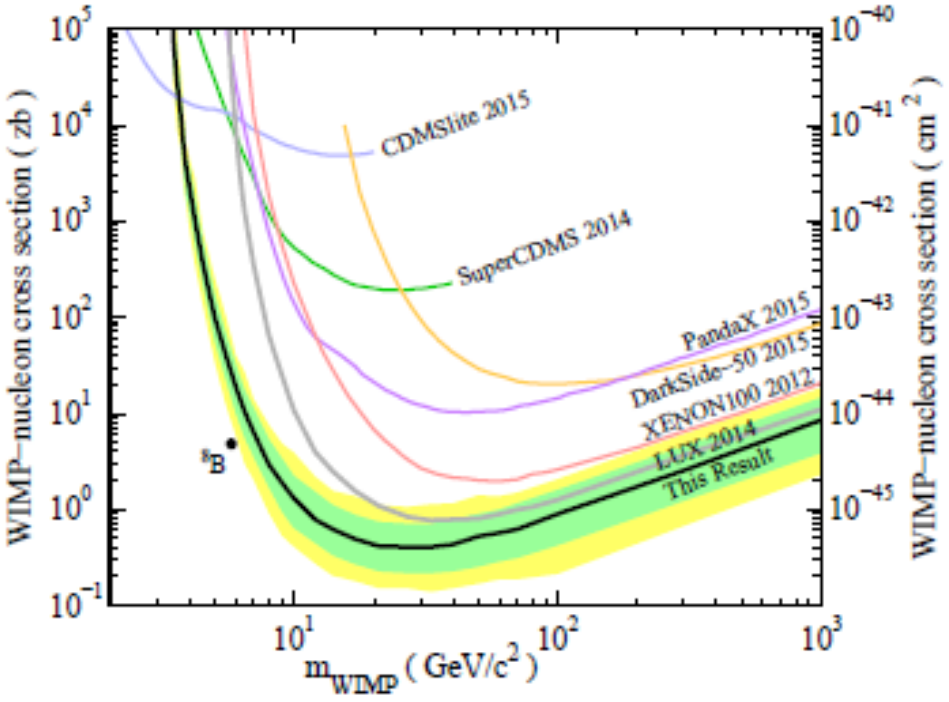

FIG. 3. Upper limits on the spin-independent elastic WIMP-nucleon cross section at 90% CL. Observed limit in black, with the 1- and 2-σ ranges of background-only trials shaded green and yellow. Also shown are limits from the first LUX analysis [6] (gray), SuperCDMS [35] (green), CDMSlite [36] (light blue), XENON100 [37] (red), DarkSide-50 [38] (orange), and PandaX [39] (purple). The expected spectrum of coherent neutrino-nucleus scattering by ^{8}B solar neutrinos can be fit by a WIMP model as in [40], plotted here as a black dot.

Experimental data that must be explained and fitted by MOG:

1. Planck and WMAP cosmic microwave background (CMB) data:
   Structure growth producing stars and galaxies.
   Angular acoustical power spectrum.
   Matter power spectrum.
   Accelerated expansion of the universe.

2. Galaxy rotation curves and galaxy evolution and stability.
3. Galactic cluster dynamics.

4. Bullet Cluster 1E0657-558 and Abell 520 cluster “train wreck” collision.

5. Gravitational lensing .
6. Binary pulsar timing (PSR 1913+16 – Hulse-Taylor binary pulsar).

7. Solar system experiments:
   Weak equivalence experiments, light deflection by Sun, Shapiro time delay (Cassini probe), planetary orbits.

8. Strong gravity: Event Horizon Telescope black hole observations.

MOG Field Equations (JCAP 0603 004 (2006), arXiv:gr-qc/0506021)

The MOG action is given by

$$S = S_G + S_\phi + S_S + S_M$$

where

$$S_G = \frac{1}{16\pi}\int d^4x\sqrt{-g}\Big[\frac{1}{G}(R+2\Lambda)\Big]$$

$$S_\phi = -\int d^4x\sqrt{-g}\Big[\frac{1}{4}B^{\mu\nu}B_{\mu\nu} - V(\phi)\Big]$$

$$S_S = \int d^4x\sqrt{-g}\Big[\frac{1}{G^3}\Big(\frac{1}{2}g^{\mu\nu}\nabla_\mu G\nabla_\nu G - V(G)\Big) + \frac{1}{\mu^2 G}\Big(\frac{1}{2}g^{\mu\nu}\nabla_\mu\mu\nabla_\nu\mu - V(\mu)\Big)\Big]$$

$$B_{\mu\nu} = \partial_\mu\phi_\nu - \partial_\nu\phi_\mu$$

S_M denotes the matter field action.

The action for a point particle test particle is

$$S_{\rm tp} = -\left(m \int ds + q \int \phi_\mu u^\mu ds \right) \qquad q = \kappa m = \sqrt{\alpha G_N} m$$

For the weak spherically symmetric field solution (Q > 0):

$$\phi_0(r) = -Q \frac{\exp(-\mu r)}{r} \qquad Q = \kappa M = \sqrt{\alpha G_N} M$$

Test particle equation of motion:

$$\frac{du^\mu}{ds} + \Gamma^\mu{}_{\alpha\beta} u^\alpha u^\beta = \frac{q}{m} B^\mu{}_\nu u^\nu \qquad \frac{d^2 r}{dt^2} + \frac{GM}{r^2} = \frac{qQ}{m} \frac{\exp(-\mu r)}{r^2} (1 + \mu r)$$

Modified acceleration law:

$$a(r) = -\frac{G_N M}{r^2} \left[1 + \alpha - \alpha \exp(-r/r_0) \left(1 + \frac{r}{r_0} \right) \right]$$

$$qQ/m = \kappa^2 M = \alpha G_N M \text{ and } G = G_N(1+\alpha) \qquad r_0 = 1/\mu$$

The field equations are given by

$$G_{\mu\nu} + \Lambda g_{\mu\nu} = -8\pi G T_{\mu\nu},$$

$$\nabla_\mu B^{\mu\nu} + \mu^2 \phi^\nu - \frac{\partial V(\phi_\mu)}{\partial \phi_\nu} = 4\pi J^\nu,$$

$$\nabla^\nu \nabla_\nu G = \frac{3}{2}\frac{\nabla^\nu G \nabla_\nu G}{G} - \frac{1}{2} G \frac{\nabla^\nu \mu \nabla_\nu \mu}{\mu^2} - \frac{3}{G} V(G) + V'(G) - G\frac{V(\mu)}{\mu^2} - \frac{1}{4\pi}(R + 2\Lambda),$$

$$\nabla^\nu \nabla_\nu \mu = \frac{\nabla^\nu \mu \nabla_\nu \mu}{\mu} + \frac{\nabla^\nu G \nabla_\nu \mu}{G} - \frac{1}{4\pi} G \mu^3 \phi^\mu \phi_\mu - \frac{2}{\mu} V(\mu) + V'(\mu).$$

The current density J^μ and energy-momentum tensor are defined by

$$J^\mu = \kappa \rho u^\mu \qquad \kappa = \sqrt{\alpha G_N}$$

$$T_{\mu\nu} = T_{M\mu\nu} + T_{\phi\mu\nu} + T_{S\mu\nu} + T_{EM}$$

$$T_{X\mu\nu} = -\frac{2}{\sqrt{-g}} \frac{\delta S_X}{\delta g^{\mu\nu}}, \quad (X = [M, \phi, S, EM]).$$

The modified weak field Newtonian potential is given by

$$\Phi(r) = -\frac{G_N M}{r}\left[1 + \alpha - \alpha e^{-\mu r}\right]$$

For an extended distribution of matter:

$$\nabla^2\Phi(\mathbf{r}) = 4\pi G_N \rho(\mathbf{r}) + \alpha\mu^2 G_N \int \frac{e^{-\mu|\mathbf{r}-\tilde{\mathbf{r}}|}}{|\mathbf{r}-\tilde{\mathbf{r}}|}\rho(\tilde{\mathbf{r}})\; d^3\tilde{\mathbf{r}}$$

A photon follows a null-geodesic path:

$$\tilde{k}^\mu \tilde{\nabla}_\mu \tilde{k}^\nu = 0 \qquad \frac{d\tilde{k}^\mu}{d\lambda} + \tilde{\Gamma}^\nu_{\alpha\beta}\tilde{k}^\alpha\tilde{k}^\beta = 0$$

k^μ = photon momentum

$$S_\chi = \int d^4x\sqrt{-g}\left(\frac{1}{2}g^{\mu\nu}\nabla_\mu\chi\nabla_\nu\chi - V(\chi)\right)$$

where $1/G = \chi^2/2.$ We couple the conformal metric $\tilde{g}_{\mu\nu}$ to the electromagnetic field $F_{\mu\nu}$ (JWM, arXiv:1410.2464 [gr-qc]):

$$\tilde{g}_{\mu\nu} = A^2(\chi)g_{\mu\nu}, \quad \tilde{g} = \mathrm{Det}\tilde{g}_{\mu\nu} = A^8(\chi)g$$

$$\tilde{\Gamma}^\alpha_{\delta\gamma} = \frac{1}{2}\tilde{g}^{\alpha\beta}(\partial_\gamma\tilde{g}_{\delta\beta} + \partial_\beta\tilde{g}_{\delta\gamma} - \partial_\delta\tilde{g}_{\beta\gamma})$$

The conformal coupling to the EM energy-momentum tensor is through the effective gravitational coupling $\tilde{G} = C(\chi(\rho))G$ where

$$\tilde{G} = C(\alpha(\rho))G_N(1+\alpha) \qquad \alpha = \frac{(G_\infty - G_N)}{G_N}$$

For a point mass M the effective screening gravitational potential experienced by the photon is

$$\Phi_{\mathrm{eff}} = \frac{\tilde{G}(\chi(\rho))M}{r} = \frac{G_N M}{r}[1 + 2h^2(\chi)\exp(-\mu_\chi r)]$$

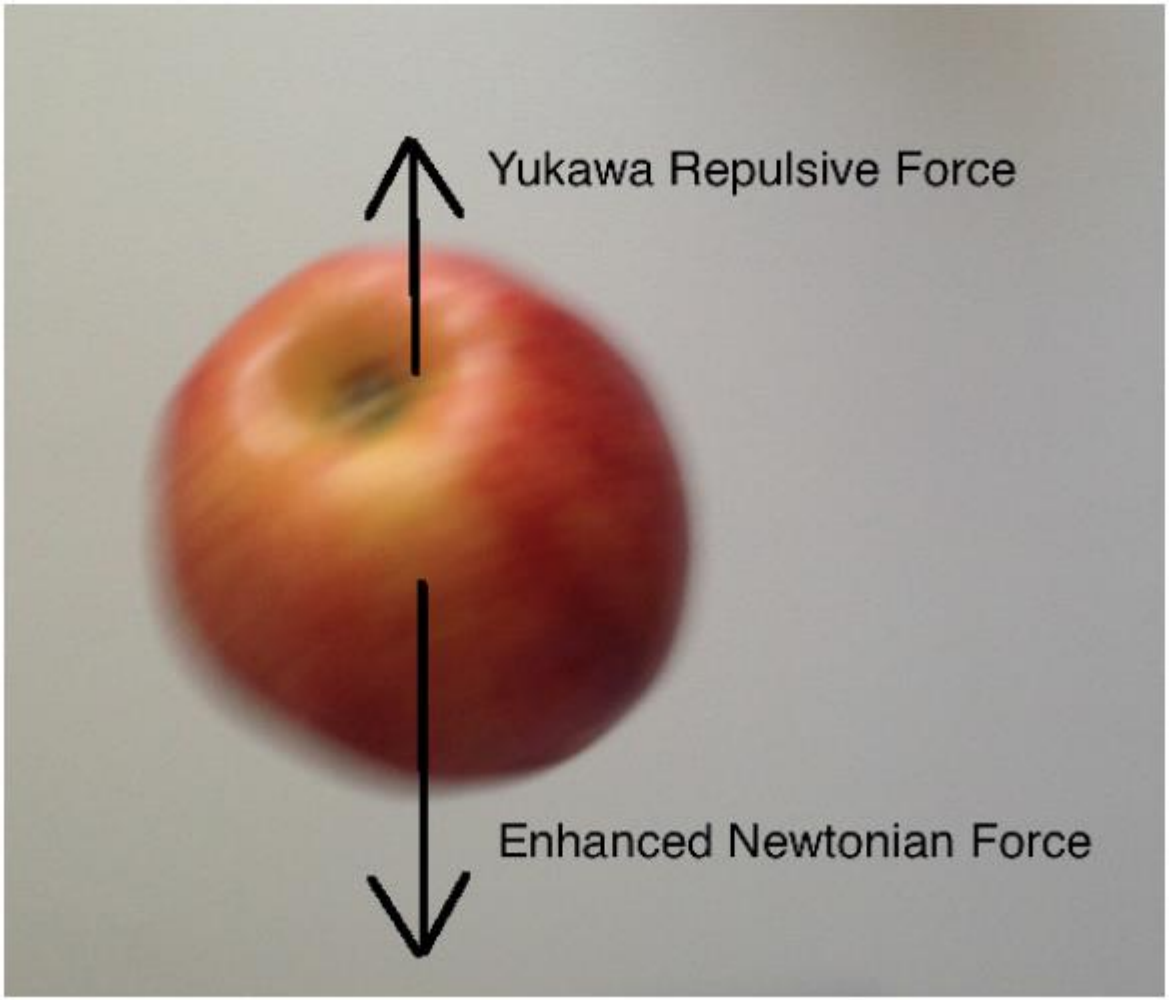

Credit: Picture is taken by Sepehr Rahvar

An alternative formulation of MOG is based on Renormalization Group Flow (JWM:arXiv:1505.05869).

The gravitational constant G in the action S is defined in terms of the "bare" Newtonian constant G_N:

$$G=G_N Z$$

The field equations derived from the action are given by

$$G_{\mu\nu} - \Lambda g_{\mu\nu} = 8\pi G T_{\mu\nu}$$

$$\nabla_\nu B^{\mu\nu} + \frac{\partial V(\phi_\mu)}{\partial \phi_\mu} = -4\pi J^\mu$$

$$\nabla_\sigma B_{\mu\nu} + \nabla_\mu B_{\nu\sigma} + \nabla_\nu B_{\sigma\mu} = 0$$

$$\nabla_\nu T^{\mu\nu} = 0.$$

As in particle physics QFT, we do not promote G, Q and μ to dynamical fields.

We implement the running of the effective G and the $\alpha = Q^2/4\pi$ ($Q = (\alpha G_N)^{1/2} M$) by using Renormalization Group (RG) flow arguments in which the "classical" coupling constants G and Q possess a scale dependent running behavior obtained by solving appropriate RG flow equations. We postulate scale dependent effective actions $\Gamma_k\{g]$ and $\Gamma_k[\phi]$, corresponding to "course-grained" free energy functionals, which define an effective field theory valid at the scale k or length l = 1/k.

Both G(k) and Q(k) are determined by the running of $\alpha(k)$:

$$k\frac{d}{dk}\alpha(k) = \beta_\alpha(\alpha, \lambda, \bar{\mu})$$

Every solution G(k), α(k), λ(k), μ(k) of the truncated flow equations is associated with the family of action functionals:

$$\Gamma_k[g,\phi] = \Gamma_k[g] + \Gamma_k[\phi].$$

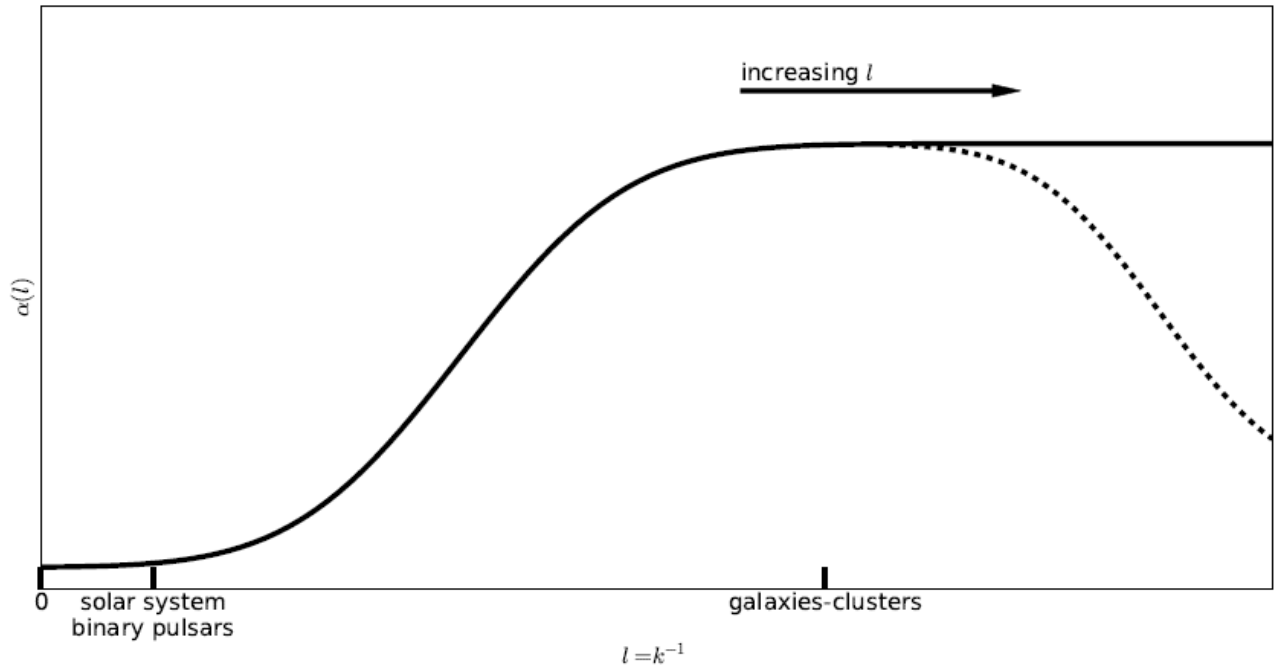

Figure 1: A schematic depiction of the running of $\alpha(\ell)$ ($\ell = k^{-1}$). The dashed curve shows the behavior of $\alpha(\ell)$ for $\alpha(\ell) \to 0$ as $\ell \to \infty$.

MOG Cosmology (JWM, arXiv:1510.07037 [astro-ph.CO])

In the present scenario there are five components to the energy density:

1. neutral pressureless phion particles (ϕ_μ field),
2. baryonic matter,
3. photons,
4. neutrinos,
5. Dark energy

Thus, we have

$$\rho = \rho_m + \rho_r + \rho_d,$$

where

$$\rho_m = \rho_b + \rho_\phi + \rho_G + \rho_\mu, \quad \rho_r = \rho_\gamma + \rho_\nu$$

and where $\rho_r, \rho_d, \rho_\gamma$ and ρ_ν denote the radiation, dark energy, photon and neutrino densities, respectively.

We assume that when ρ_ϕ dominates in the early universe before decoupling $\alpha < 1$.

$$G \sim G_\infty \sim G_N$$

Big bang at t = 0 followed by either inflationary expansion period or by variable speed of light (VSL) with $c > c_0$ (c_0 = measured speed of light today).

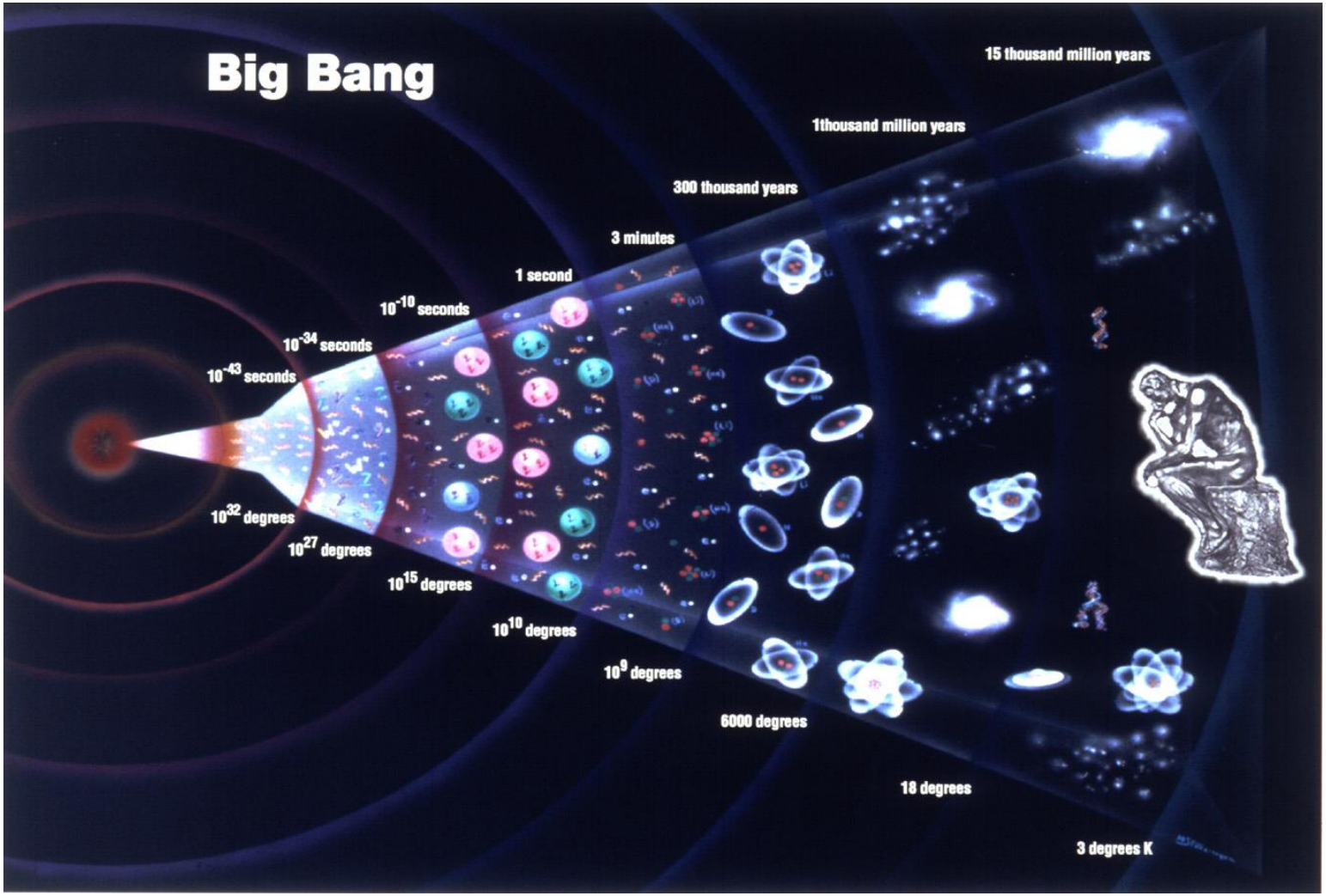

At the time of big-bang-nucleosynthesis (BBN), we have $G \sim G_N$, guaranteeing that the production of elements agrees with observation. After decoupling $\rho_\phi \sim \rho_b$ until stellar and galaxy formation when $\rho_\phi \ll \rho_b$ and the MOG non-relativistic acceleration law sets in to explain the rotation curves of galaxies and the dynamics of clusters in the present universe without detectable dark matter.

We assume that at horizon entry until some time after decoupling:

$$\rho_\phi \gg \rho_b,\ \rho_\phi \gg \rho_G,\ \rho_\phi \gg \rho_\mu$$

and $V_G = V_\mu = 0$. The first Friedman equation becomes

$$H^2 = \frac{8\pi G_N \rho_\phi}{3} + \frac{\Lambda}{3} \qquad \rho_\phi = \frac{1}{2}\omega\mu^2\phi_0^2$$

The Jeans equation for density perturbations is

$$\ddot{\delta}_{\mathbf{k}} + 2H\dot{\delta}_{\mathbf{k}} + \left(\frac{c_s^2 a_0^2 k^2}{a^2} - 4\pi G_N \bar{\rho}\right)\delta_{\mathbf{k}} = 0 \qquad c_s = \sqrt{\frac{dp}{d\rho}}$$

The Proca vector field ϕ_μ is a neutral massive spin 1 particle (massive hidden photon). Because it does not couple to massless photons, it can be treated as almost pressureless. The pressure gradient term in the Jeans equation is absent and the speed of sound is zero, $c_s \sim 0$. We get

$$\ddot{\delta}_{\mathbf{k}} + 2H\dot{\delta}_{\mathbf{k}} - 4\pi G_N \bar{\rho}\delta_{\mathbf{k}} = 0$$

There is no oscillatory behavior of the phion particles and perturbations grow at all wave lengths. On the other hand, the baryon perturbations oscillate before decoupling, due to the photon-baryon pressure, producing baryon acoustical oscillations.

After decoupling the baryon density perturbations grow and catch up with the phion $\delta\rho_b$ density perturbations. The phion density perturbations solve the problem of getting sufficient growth to form stars and galaxies later in the universe.

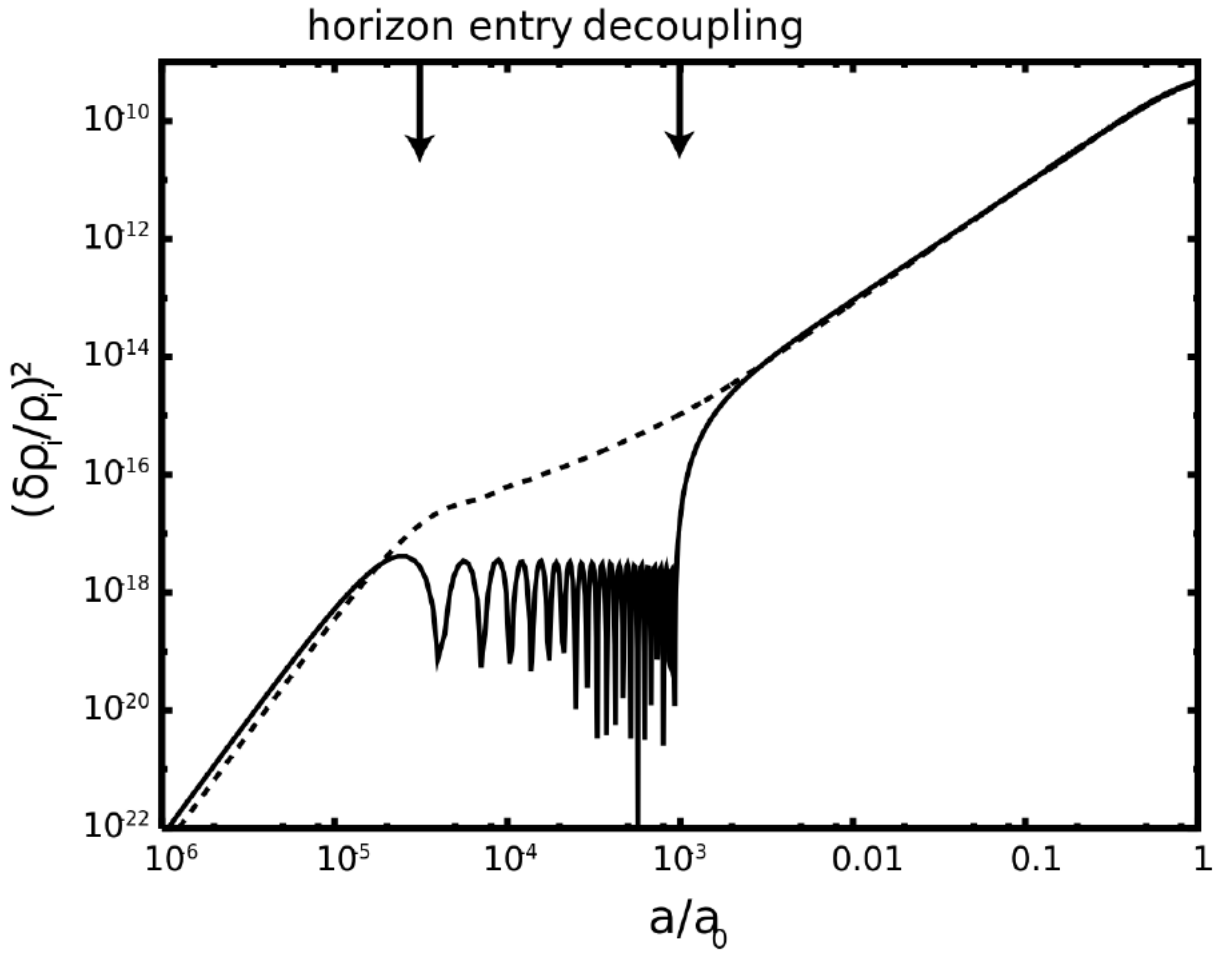
horizon entry
decoupling
10^{10}
10^{12}
10^{14}
10^{16}
10^{18}
10^{20}
10^{22}
$(\delta\rho_i/\rho_i)^2$
10^6
10^5
10^4
10^3
0.01
0.1
1
a/a_0

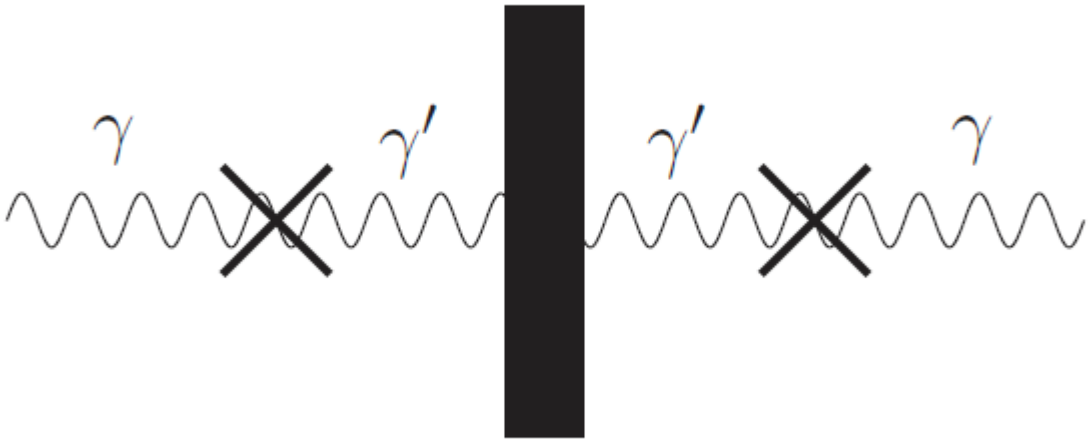

Schematic picture of a "light shining through a wall" experiment. The crosses denote the non-diagonal mass terms that convert photons into dark Proca (massive) photons. The photon γ oscillates into the dark photon γ' and, after the wall, back into the photon γ which can then be detected.

Consider a U(1) neutral ϕ_μ hidden massive photon, in addition to the usual $U(1)_{QED}$ photon. The most general renormalizable Lagrangian for the vector field ϕ_u sector and for weak gravitational fields is

$$\mathcal{L}_\phi = -\frac{1}{4}F^{\mu\nu}F_{\mu\nu} - \frac{1}{4}B^{\mu\nu}B_{\mu\nu} - \frac{1}{2}\chi F^{\mu\nu}B_{\mu\nu} + \frac{1}{2}m_{\gamma'}^2\phi_\mu\phi^\mu$$

where $F_{\mu\nu}$ is the electromagnetic field strength (J. Jaeckel and A. Ringwald, Phys. Lett. B659: 509 (2008), arXiv:0707.3063 [hep-ph]).

As the universe expands beyond the time of decoupling, the gravitational attraction between baryons increases and $G = G_\infty = G_N(1+\alpha)$. Eventually, as the large scale structures form $\rho_\phi < \rho_b$ and the baryon dominated MOG takes over. The galaxy rotation curves and the galactic cluster dynamics are determined without dark matter. The best fit values for α and μ are:

$$\alpha = 8.89 \pm 0.34 \qquad \mu = 0.04 \pm 0.004\,\mathrm{kpc}^{-1}$$

The phion mass parameter is a scalar field which evolves with time as the universe expands. After horizon entry $m_\phi \gg 10^{-28}\,\mathrm{eV}$ and the phion particle behaves like cold dark matter (CDM). When the earliest stars and galaxies form, the phion mass undergoes a significant decrease. In the present universe from the best fit value $\mu = 0.04\,\mathrm{kpc}^{-1}$ we get $m_\phi = 2.6 \times 10^{-28}\,\mathrm{eV}$. The phion (hidden photon) mass becomes ultra-light and cannot contribute to the dynamics of galaxies and galactic clusters.

We conclude that dark matter particles cannot be detected in the present universe, either by laboratory experiments or in astrophysical observations (Pamela, AMS, gamma ray bursts).

The acoustical angular power spectrum at the CMB can be calculated in MOG.

$$\Delta^2 = Ak^3T^2(k)P_0(k). \qquad T(k) = T_b(k) + T_\phi(k).$$

For a constant non-zero value of α, we have in the present universe $\rho_\phi \ll \rho_b$:

$$(G_N\rho)_{\Lambda CDM} = (G_N(1+\alpha)\rho)_{\rm MOG}. \quad \rho_{\Lambda CDM} = \rho_b + \rho_{CDM} \qquad \rho_{\rm MOG} = \rho_b$$

Now, red-shifting towards the CMB, ρ_ϕ becomes smoothly bigger than ρ_b and $\alpha << 1$:

$$(G_N\rho)_{\Lambda\rm CDM} = (G_N\rho_\phi)_{\rm MOG}$$

It follows that the angular acoustical power spectrum calculation can be duplicated in MOG using the Planck 2013 best-fit values:

$$\Omega_b h^2 = 0.022199, \quad \Omega_c h^2 = 0.11847,\ n_s = 0.9624,\ H_0 = 67.94\,{\rm km\,sec^{-1}\,Mpc^{-1}}$$

$\Omega_\Lambda = 0.6939$, $\sigma_8 = 0.8271$

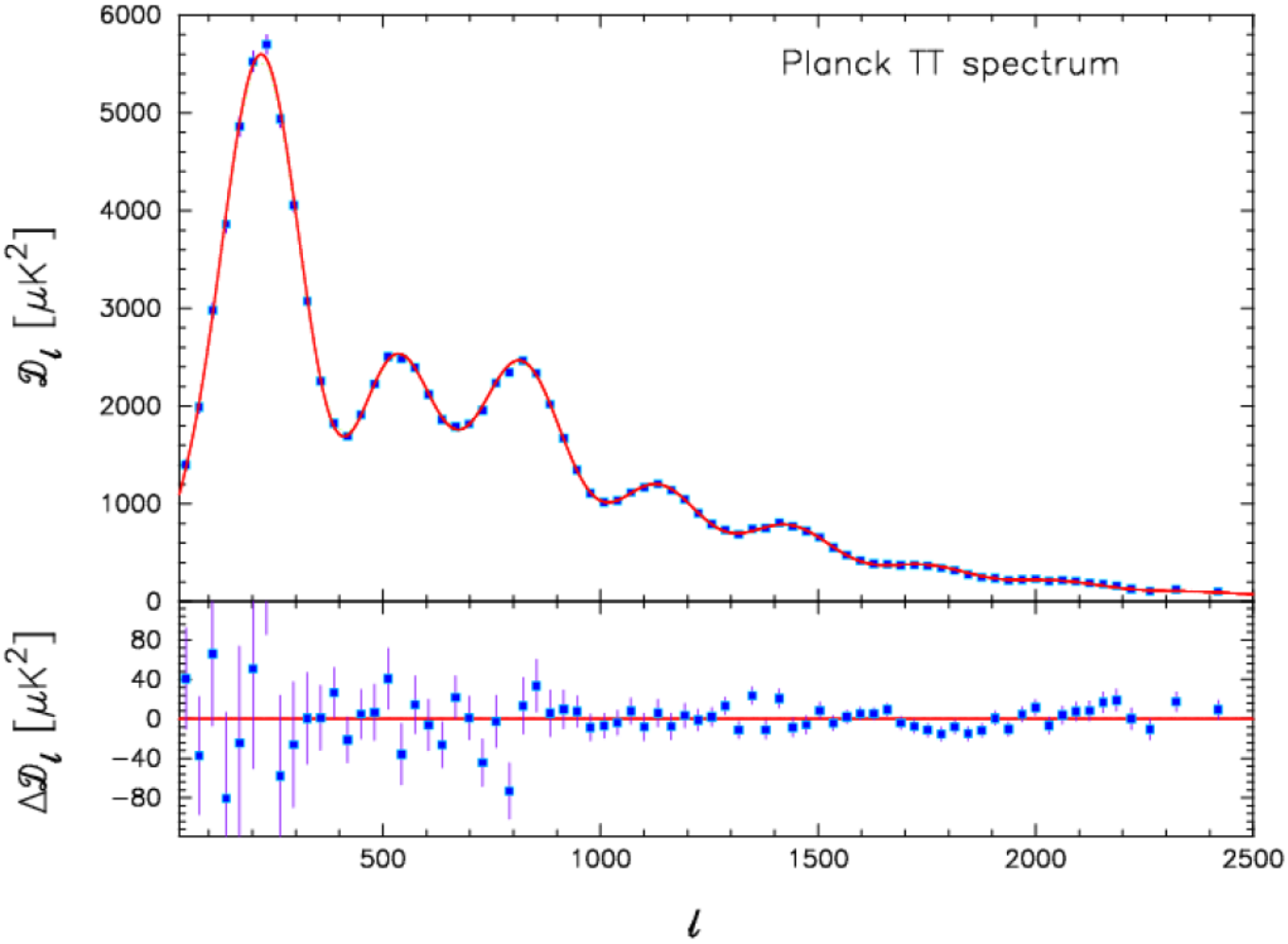
Planck TT spectrum
$\mathcal{D}_\ell$ [μK^2]
$\Delta\mathcal{D}_\ell$ [μK^2]
ℓ
6000
5000
4000
3000
2000
1000
0
80
40
0
−40
−80
500
1000
1500
2000
2500

Matter Power Spectrum

Figure 1. The matter power spectrum. Three models are compared against five data sets (see text): Λ-cold dark matter (Λ-CDM) (dashed blue line, $\Omega_b = 0.035$, $\Omega_c = 0.245$,$\Omega_\Lambda = 0.72$, $H = 71$ km/s/Mpc), a baryon-only model (dotted green line, $\Omega_b = 0.035$, $H = 71$ km/s/Mpc) and modified gravity (MOG) (solid red line, $\alpha = 19$, $\mu = 5$ h Mpc^{-1}, $\Omega_b = 0.035$, $H = 71$ km/s/Mpc), Data points are colored light blue [Sloan Digital Sky Survey (SDSS) 2006], gold (SDSS 2004), pink [Two-degree-Field (2dF)], light green [UK Schmidt Telescope (UKST)] and dark blue (CfA).

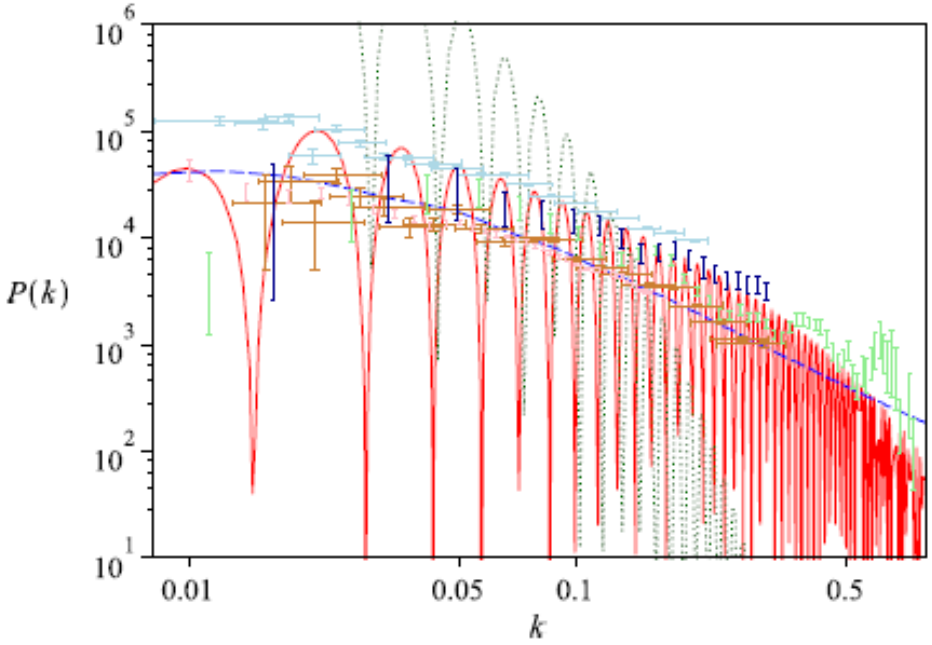

The matter power spectrum determined by the distribution of matter obtained from large scale galaxy surveys can also be predicted by MOG. A suitable window function and an initial scale invariant power spectrum P_0 are chosen to determine P(k). Baryon unit oscillations are greatly dampened by the window function.

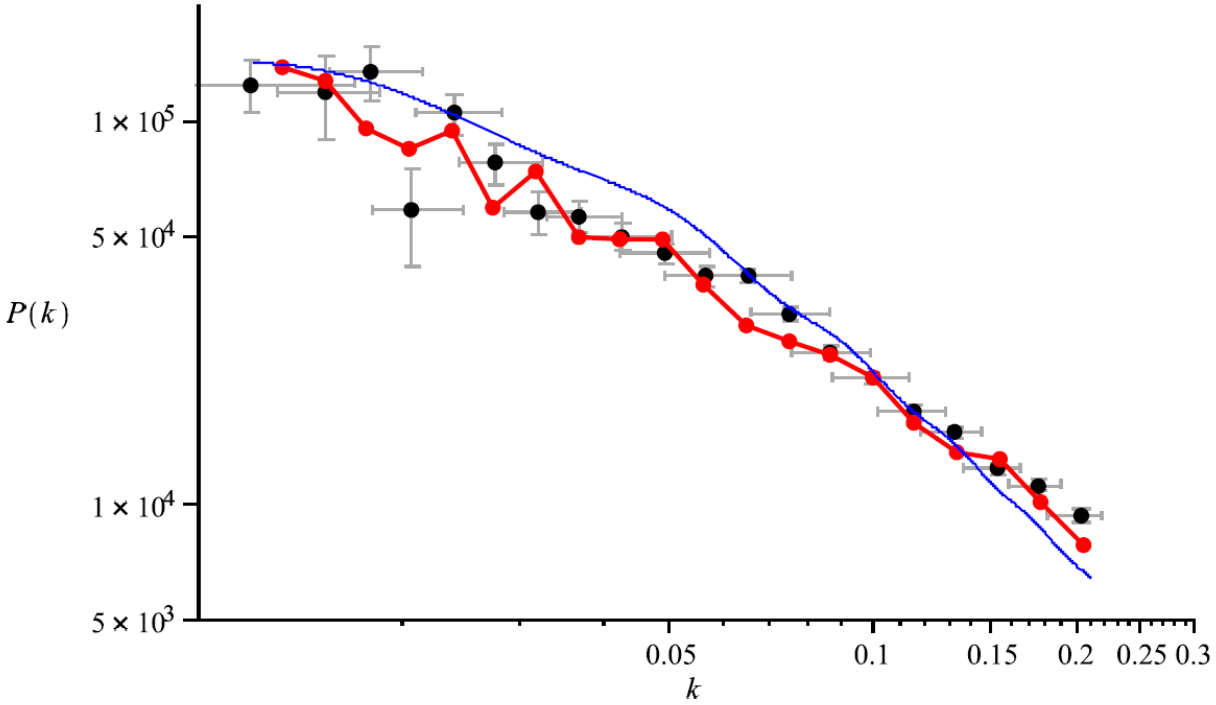

With a sufficiently large survey of galaxies, the unit baryon oscillations will begin to be observed and distinguish between MOG, without detectable dark matter, and the standard ΛCDM model without unit baryon oscillations. However, the presently observed baryon oscillations cannot be used to distinguish MOG from The ΛCDM model.

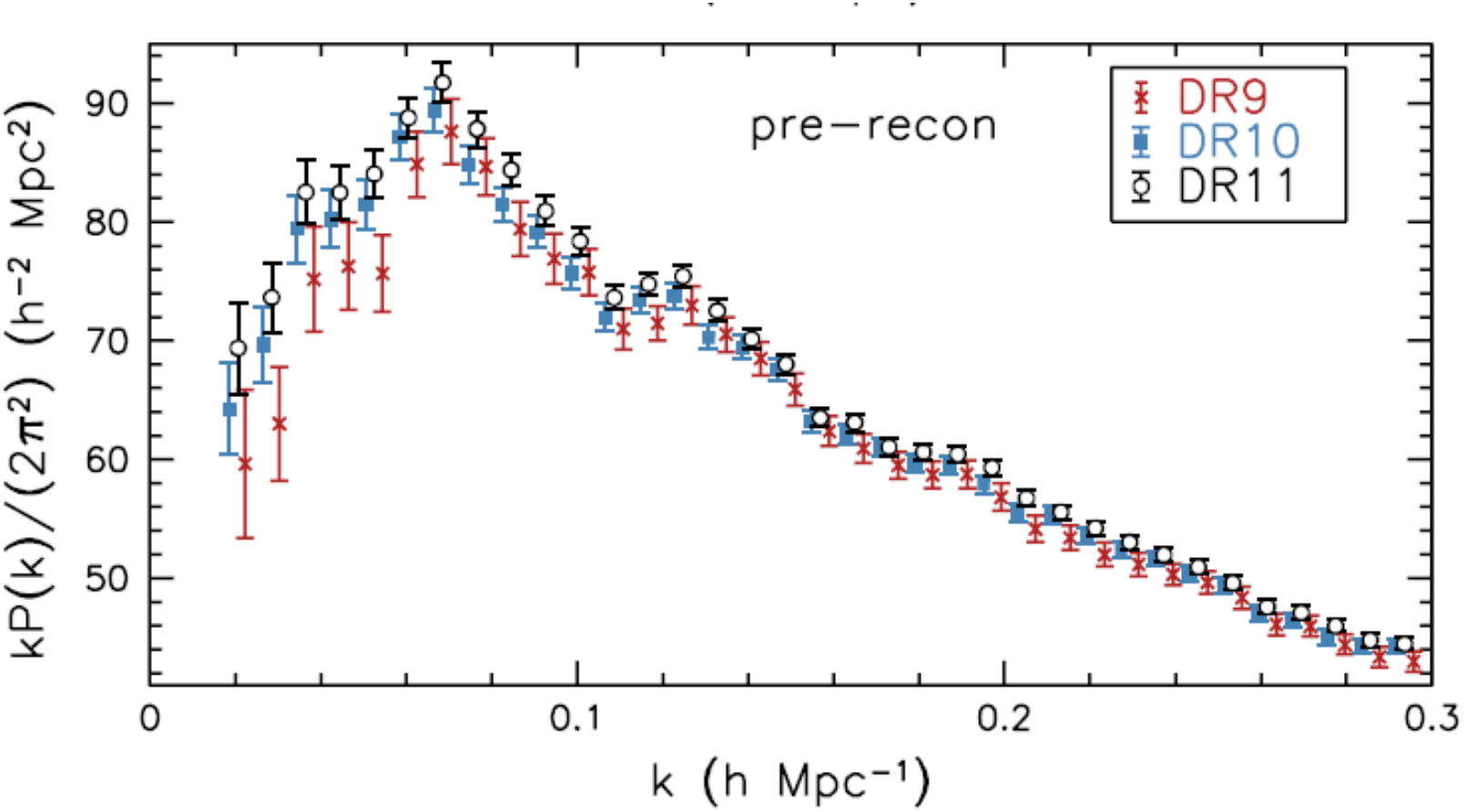

L. Anderson et al., arXiv:1312.4877

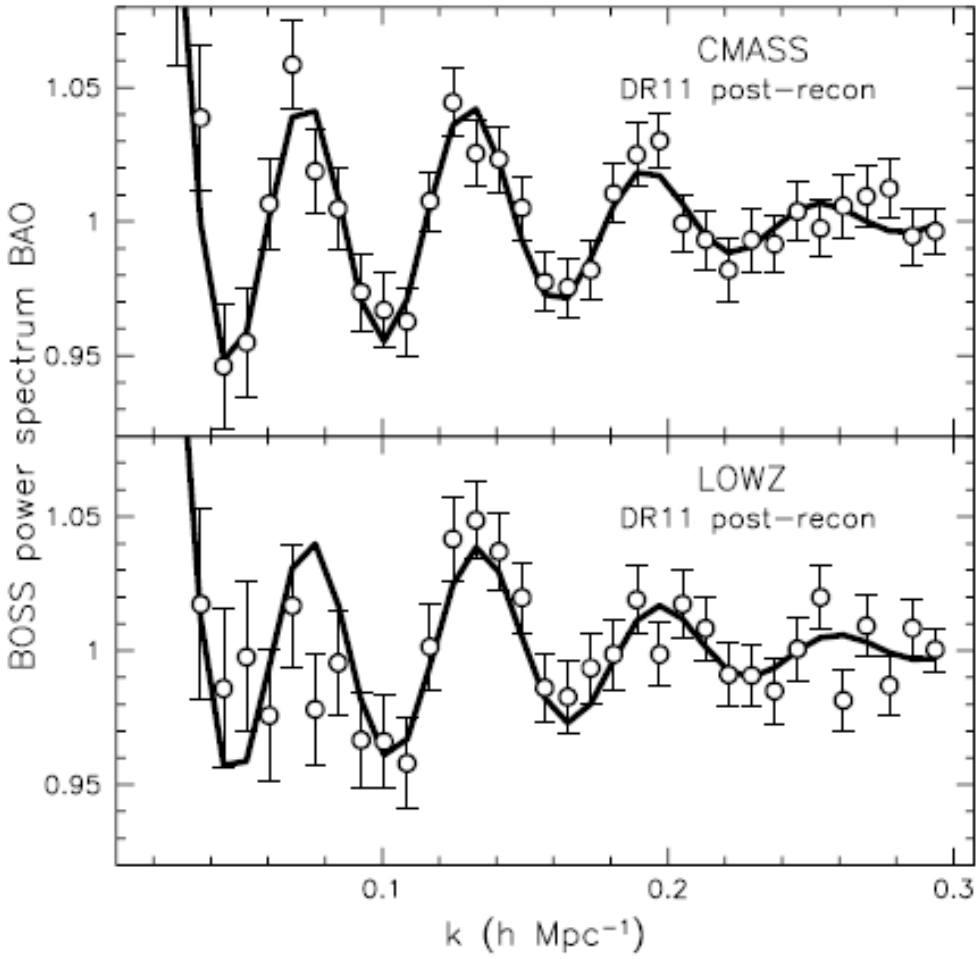

L. Anderson, arXiv:1312.4877

Rotation Curves of Galaxies (JWM and S. Rahvar, MNRAS 436, 1439 (2013), arXiv:1306.6385 [astro-ph])

We adopt the best-fitting values of α and μ and let the stellar-to-mass ratio M/L be the only free parameters and obtain fits to the Ursa Major catalogue of galaxies. The average value of χ^2 for all the galaxies is $\overline{\chi^2} = 1.07.$

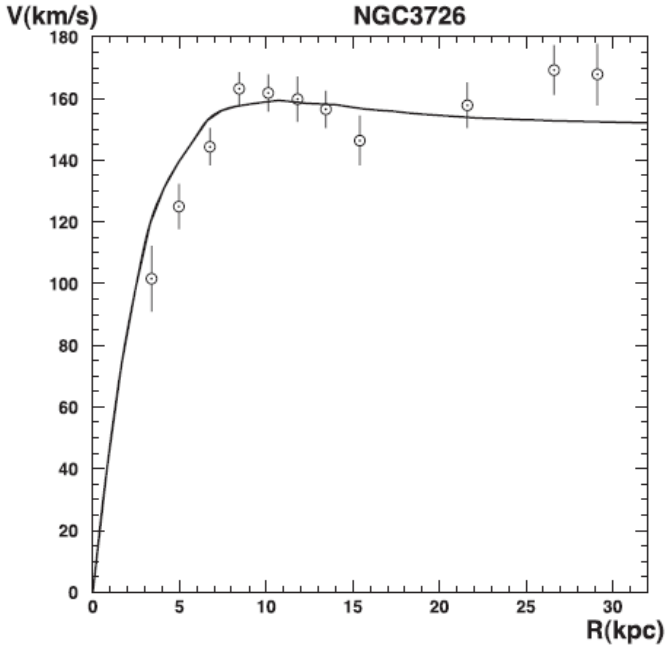

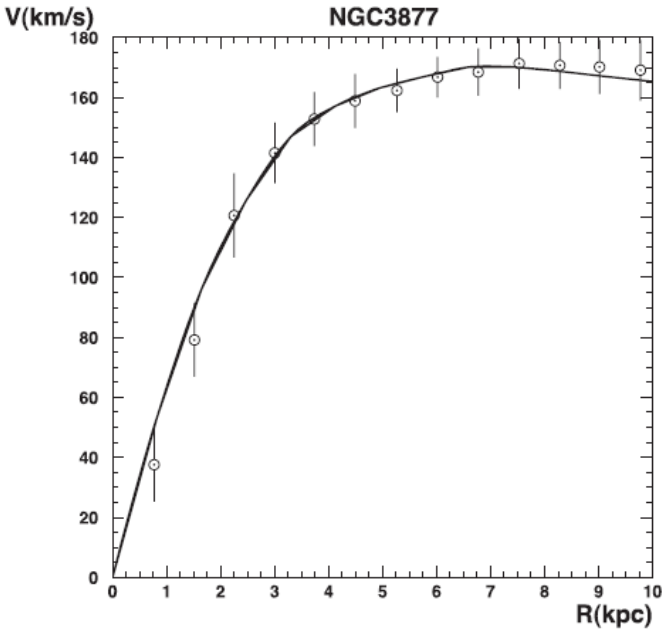

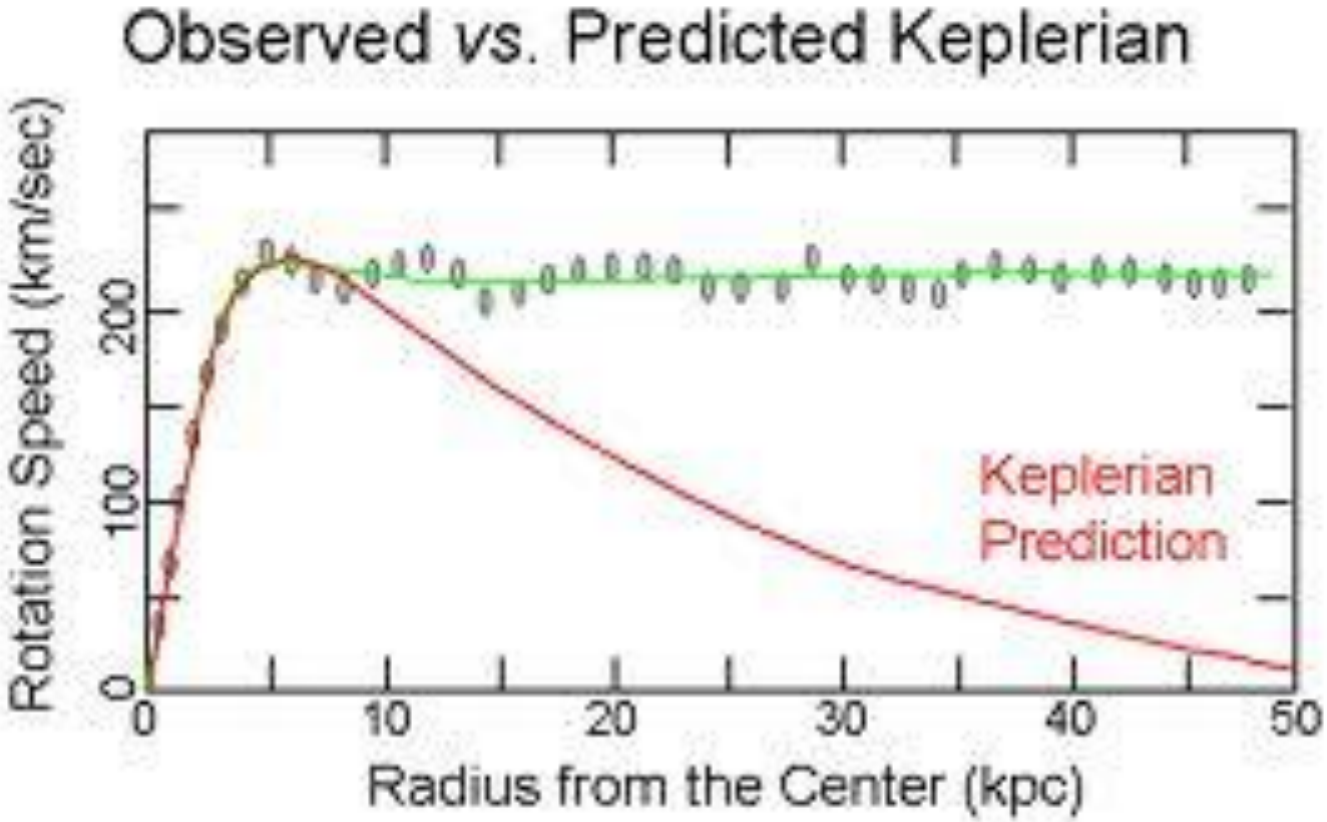
Observed vs. Predicted Keplerian
Rotation Speed (km/sec)
0
100
200
0
10
20
30
40
50
Radius from the Center (kpc)
Keplerian
Prediction

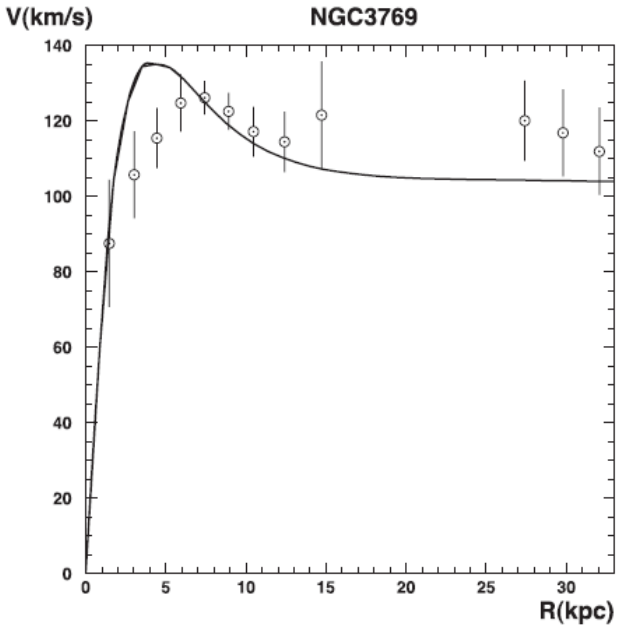
V(km/s)
NGC3769
R(kpc)

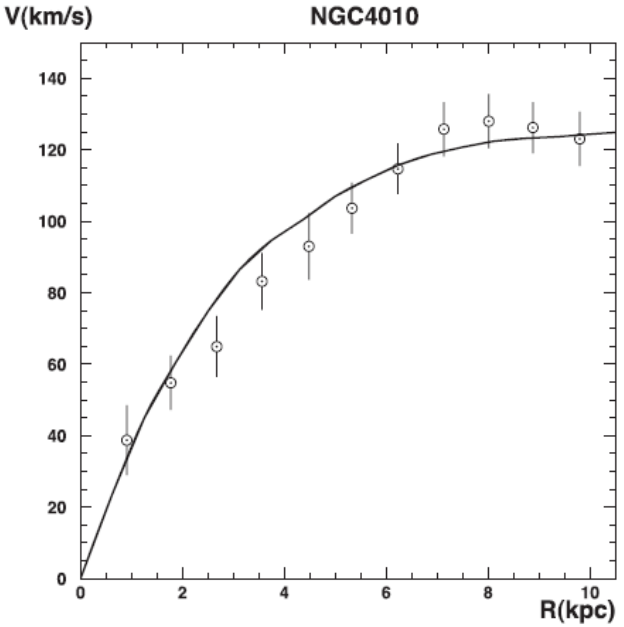
V(km/s)
NGC4010
R(kpc)

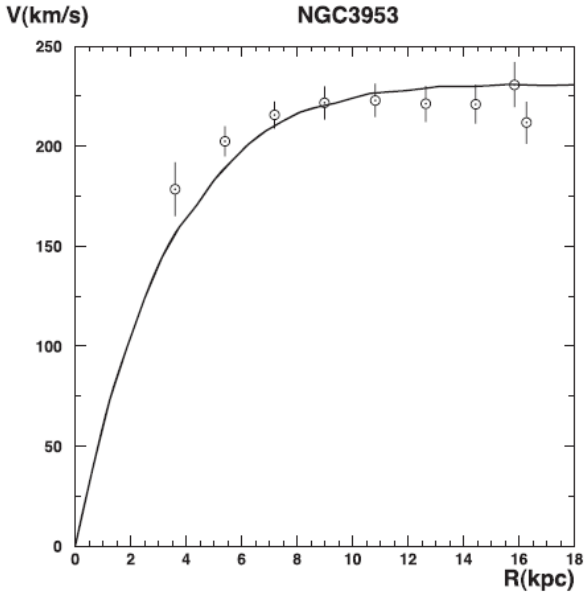
V(km/s)
NGC3953
R(kpc)

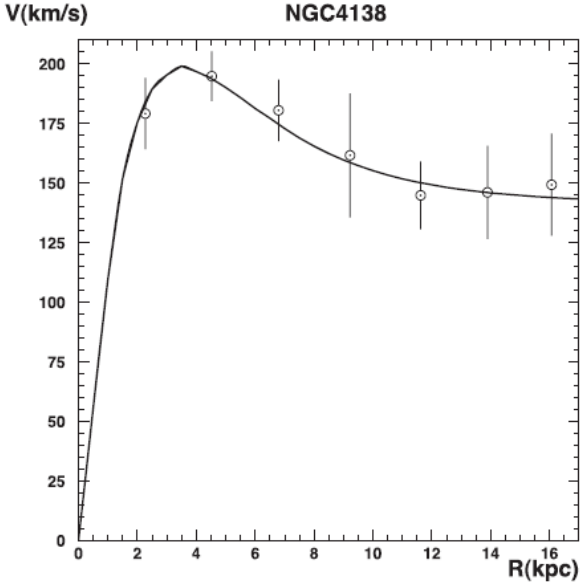
V(km/s)
NGC4138
R(kpc)

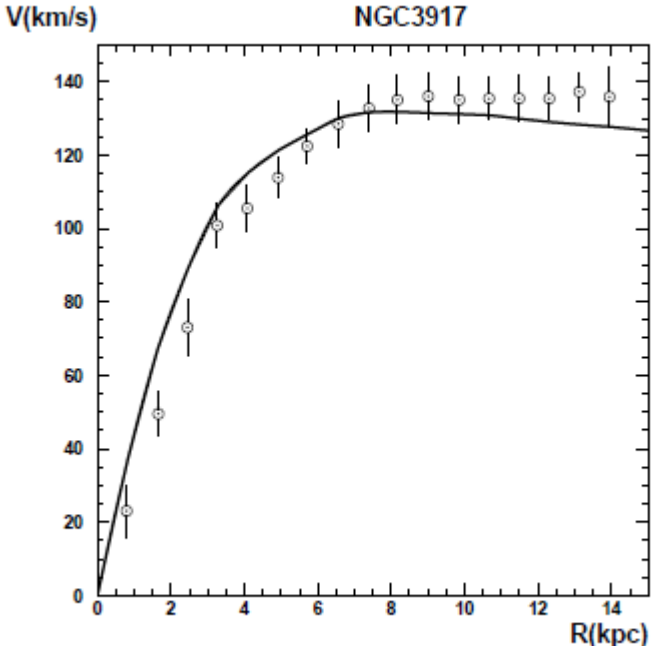
V(km/s)
NGC3917
R(kpc)

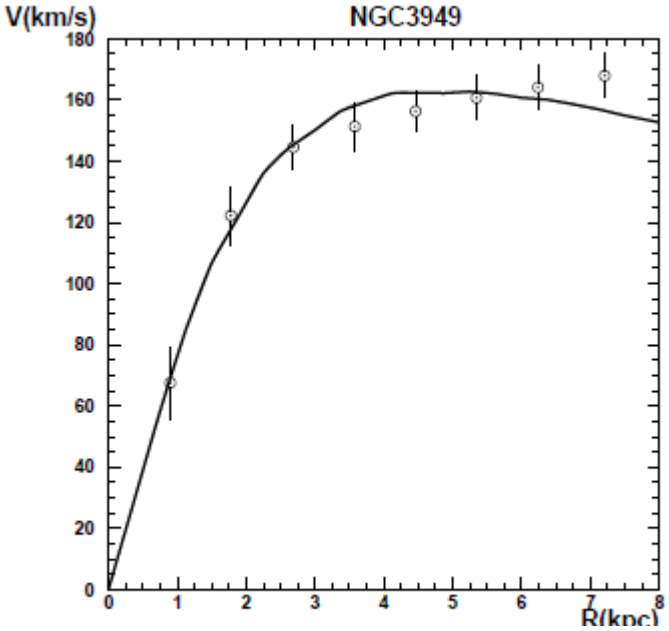
V(km/s)
NGC3949
R(kpc)

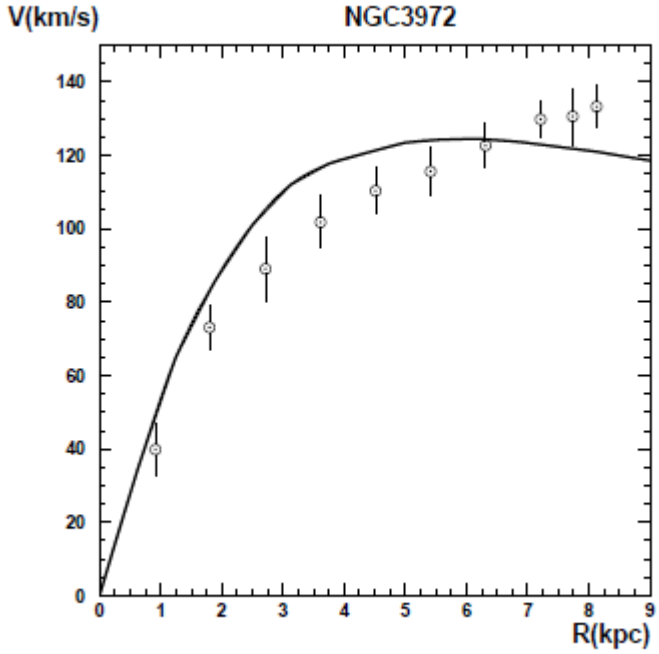
V(km/s)
NGC3972
R(kpc)

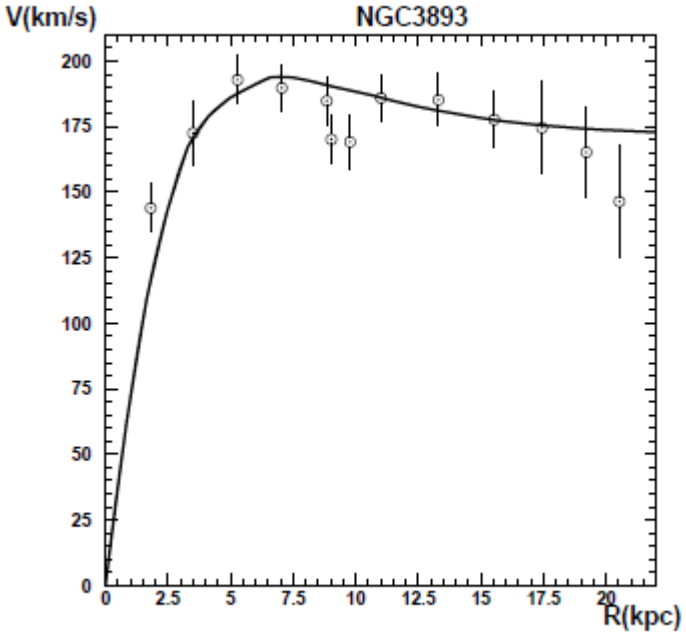
V(km/s)
NGC3893
R(kpc)

P. Battacharjee, S. Chaudhury and S. Kundu, Ap. J. 785, 63 (2014), arXiv:1310.2559

J. W. Moffat and V. T. Toth, Phys. Rev. D91, 043004 (2015), arXiv:1411.6701 [astro-ph.GA]

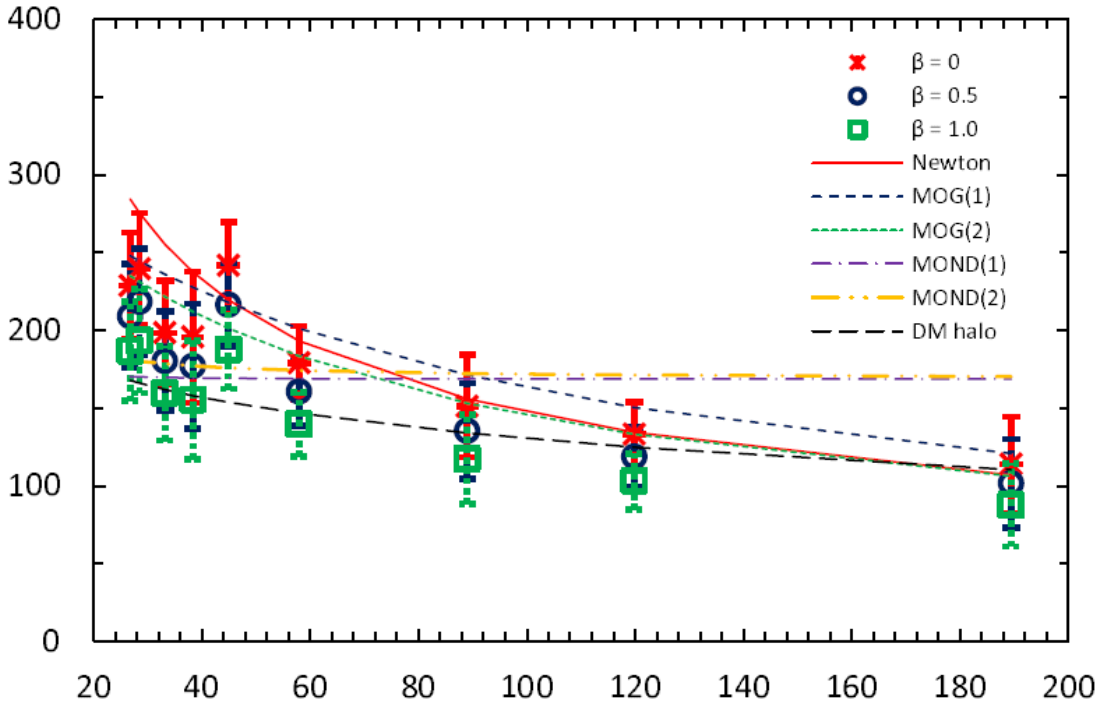

The solid red line is the Newtonian fit with a mass $M = 5 \times 10^{11} M_\odot$. The blue medium dashed and green short dashed lines correspond to MOG using the values $M = 4 \times 10^{10} M_\odot$, $\alpha = 15.01$, $\mu = 0.0313$ kpc^{-1}, and $M = 5 \times 10^{10} M_\odot$, $\alpha = 8.89$, $\mu = 0.04$ kpc^{-1}, respectively. The purple dash-dotted line is MOND with $M = 5 \times 10^{10} M_\odot$, $a_0 = 1.21 \times 10^{-8}$ cm/s^2 The black long - dashed line is the dark matter halo prediction.

We can obtain the flat rotation curves from the best fit and compare them to the observed luminosity of galaxies (Tully-Fisher relation):

$v^4 \sim M$

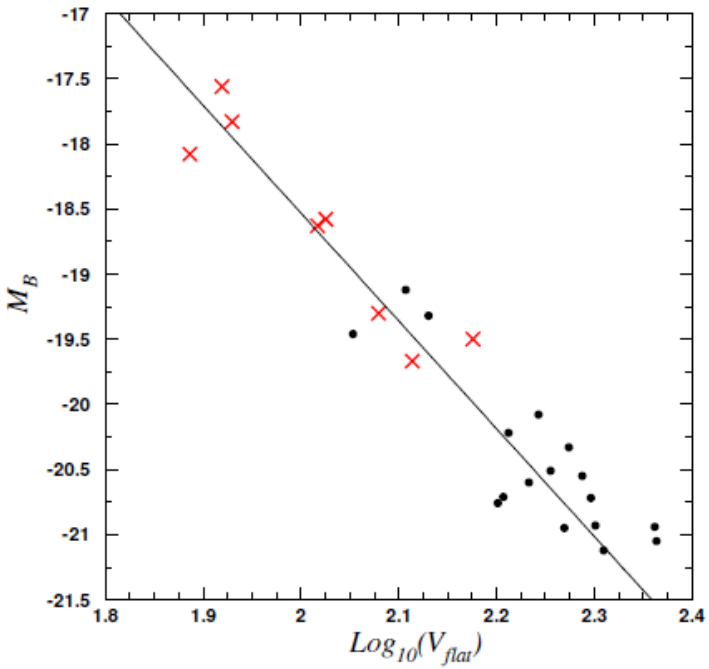

The best fit is obtained for $M = -8.27 \times \log(V_{flat}) - 1.99$

Cluster Dynamics (JWM & S. Rahvar, MNRAS, 441, 3724 (2014), arXiv:1309.5077 [astro-ph].

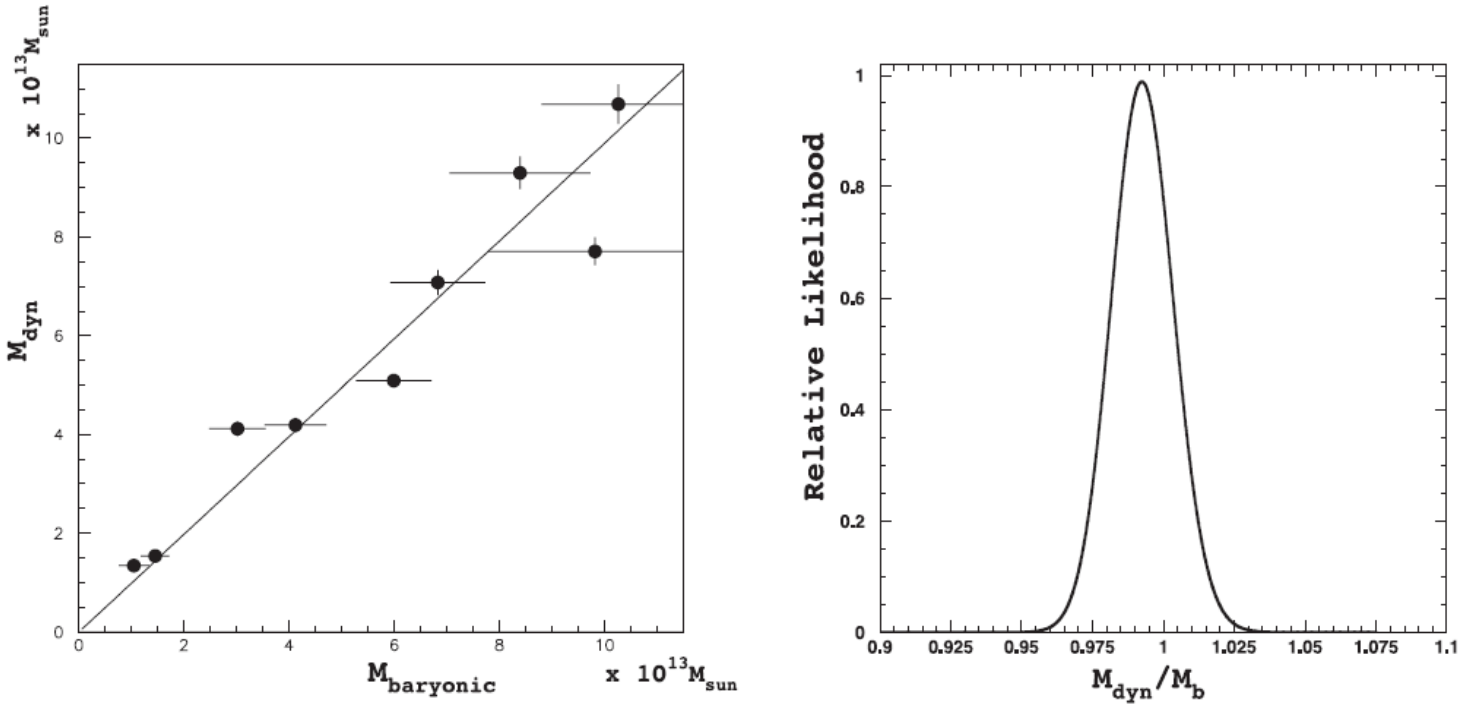

Comparison of the dynamical mass in MOG versus the baryonic mass for clusters. The baryonic mass is composed of gas and stars. The filled circles indicate the corresponding masses up to r_{500} with the corresponding error bars. The solid line shows the best fit to the linear relation $M_{\rm dyn} = \beta_{\rm cl} M_{\rm bar}$ between the two masses with the best fit value of $\beta = 0.99$. The likelihood function for this fit is given in the right-hand panel.

Bullet Cluster 1E0657-558 and Abell 520 Cluster Collisions (J. R. Brownstein and JWM, MNRAS, 382, 29 (2007), arXiv:0702146 [astro-ph]). Norman Israel and JWM, (in preparation).

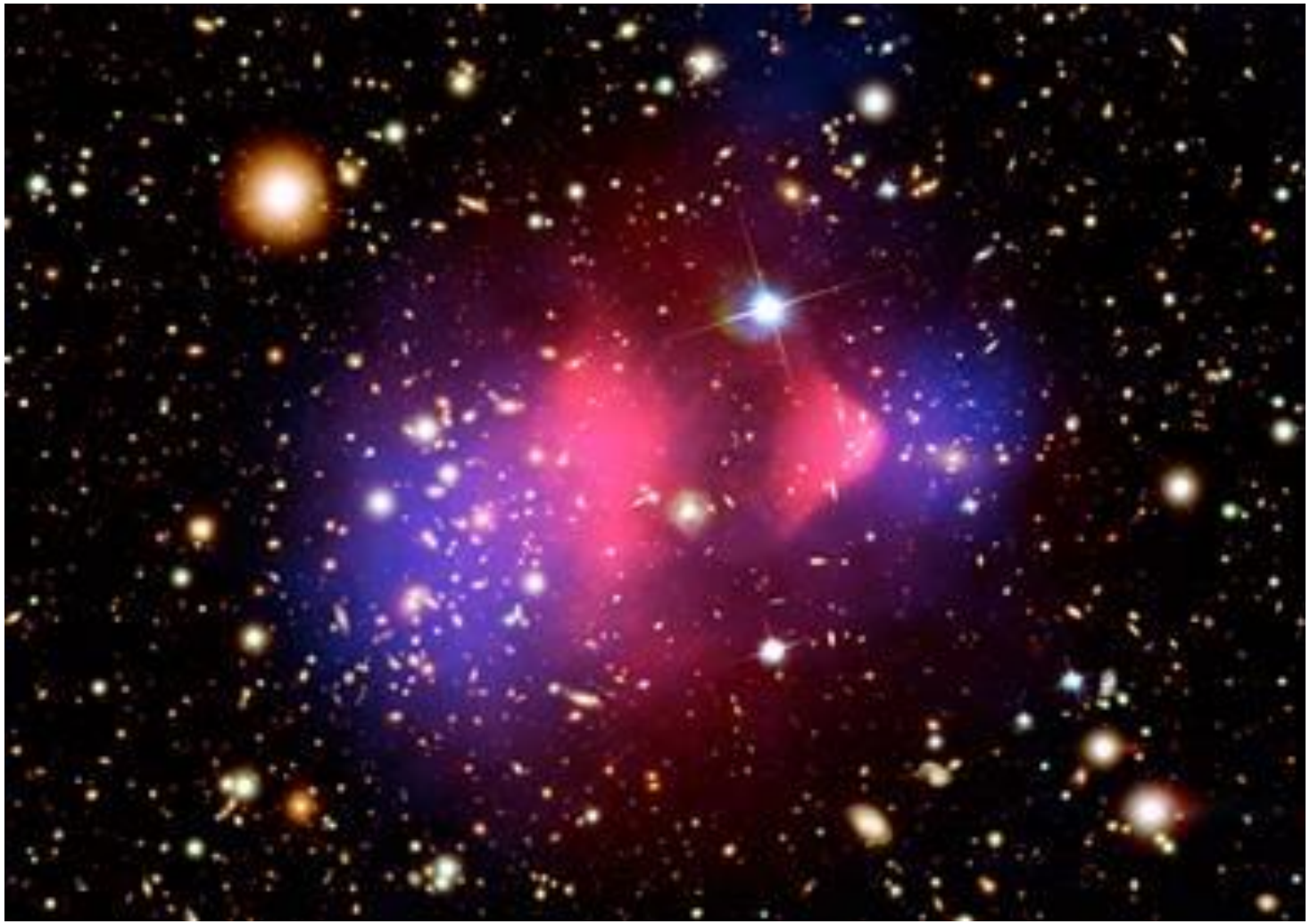

The κ –convergence predicted by MOG that accounts for the weak and strong lensing by the merging clusters accounts for the off-set of mass observed by Clowe et al. 2006. The relationship between κ and the surface density Σ is given by

$$\kappa(x,y) = \int \frac{4\pi G(r)}{c^2}\frac{D_{\rm l}D_{\rm ls}}{D_{\rm s}}\rho(x,y,z)dz \equiv \frac{\bar{\Sigma}(x,y)}{\Sigma_c},$$

where

$$\bar{\Sigma}(x,y) = \int \mathcal{G}(r)\rho(x,y,z)dz,$$

$$\mathcal{G}(r) \equiv \frac{G(r)}{G_N} = 1+\sqrt{\frac{M_0}{M(r)}}\left\{1-\exp\left(-\frac{r}{r_0}\right)\left(1+\frac{r}{r_0}\right)\right\}$$

$\alpha = \sqrt{\frac{M_0}{M(r)}}$ $\qquad \mathcal{G}_\infty = 1+\sqrt{\frac{M_0}{M}}$ = 1+ α

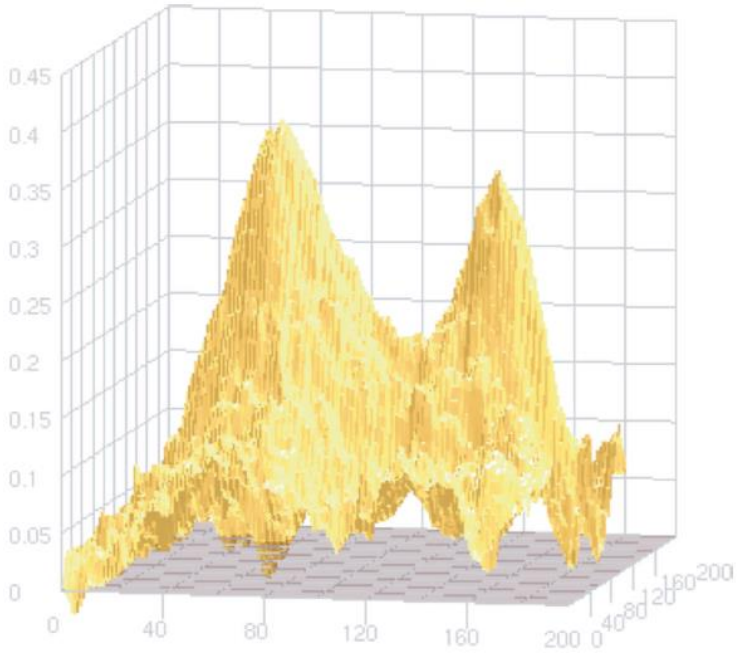

Convergence κ – map data
for Bullet Cluster (Clowe et al 2006).

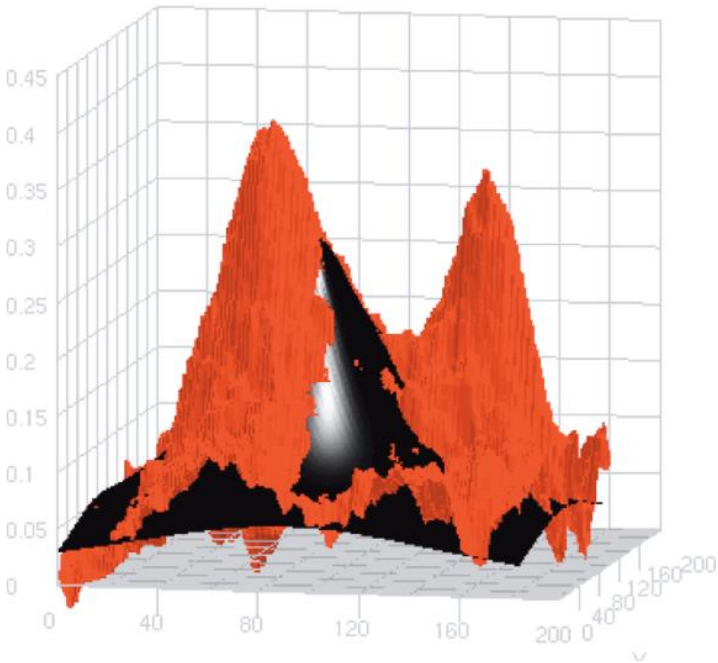

MOG prediction for κ – map convergence.

The fit to the Bullet Cluster data requires no non-baryonic dark matter!

Abell 520 a threat to dark matter models? (Jee et al., ApJ. 747, 96 (2012) arXiv:1202.6368).

Data from NASA's Chandra X-ray Observatory show the hot gas in the colliding clusters colored in green. The gas provides evidence that a collision took place. Optical data from NASA's Hubble Space Telescope and the Canada-France-Hawaii Telescope (CFHT) in Hawaii are shown in red, green, and blue. Starlight from galaxies within the clusters, derived from observations by the CFHT and smoothed to show the location of most of the galaxies, is colored orange.

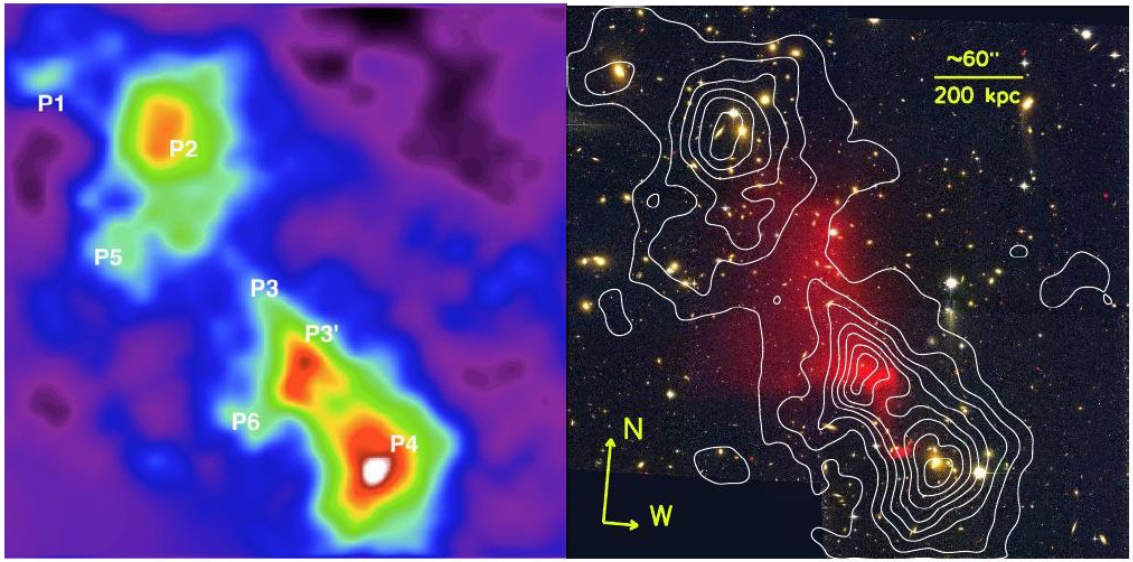

FIG. 1: A520 κ-map on x-ray [1]. The result shows that one of the peaks (P3' on left) coincide with the X-ray gas (red on right).

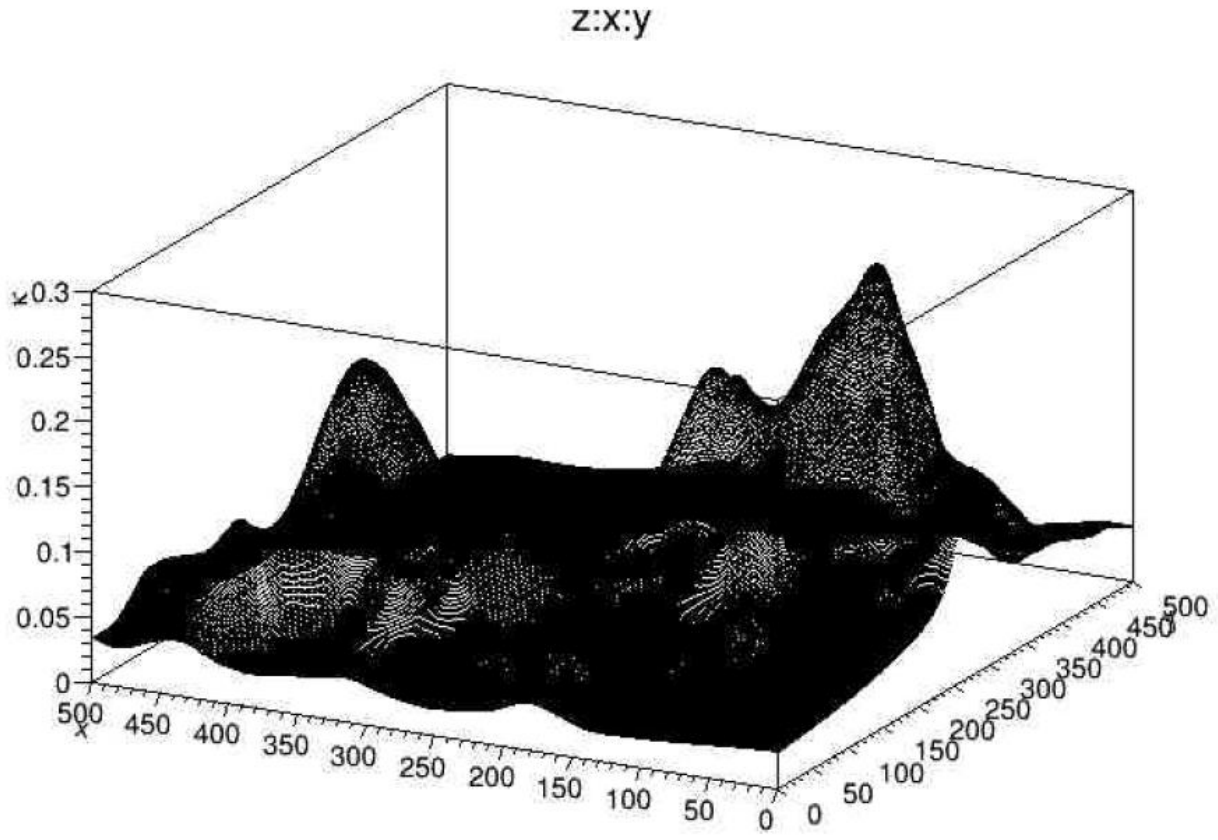
z:x:y
0.3
0.25
0.2
0.15
0.1
0.05
0
500
450
400
350
300
250
200
150
100
50
0
0
50
100
150
200
250
300
350
400
450
500

MOG Black Holes

JWM, Eur. Phys. J. C (2015) 75, 175, arXiv:1412.5424 [gr-qc] and JWM, Eur. Phys. J. C (2015) 75, 130, arXiv:1502.01677 [gr-qc]

The STVG field equations are ($T_{M\mu\nu}=0$) :

$$R_{\mu\nu} = -8\pi G T_{\phi\mu\nu}$$

We assume that $\partial_\nu G \sim 0$ and we ignore the small vector field mass $m_\phi \sim 0$:

$$m_\phi = 2.6 \times 10^{-28}\ \mathrm{eV}$$

$$T_{\phi\mu\nu} = -\frac{1}{4\pi}(B_\mu{}^\alpha B_{\nu\alpha} - \frac{1}{4} g_{\mu\nu} B^{\alpha\beta} B_{\alpha\beta}) \qquad B_{\mu\nu} = \partial_\mu \phi_\nu - \partial_\nu \phi_\mu$$

$$\nabla_\nu B^{\mu\nu} = \frac{1}{\sqrt{-g}} \partial_\nu (\sqrt{-g} B^{\mu\nu}) = 0 \qquad \nabla_\sigma B_{\mu\nu} + \nabla_\mu B_{\nu\sigma} + \nabla_\nu B_{\sigma\mu} = 0$$

The Schwarzschild-MOG and Kerr-MOG black hole metrics are

$$ds^2 = \left(1 - \frac{2G_N(1+\alpha)M}{r} + \frac{G_N^2\alpha(1+\alpha)M^2}{r^2}\right)dt^2 - \left(1 - \frac{2G_N(1+\alpha)M}{r} + \frac{G_N^2\alpha(1+\alpha)M^2}{r^2}\right)^{-1}dr^2 - r^2d\Omega^2$$

$$ds^2 = \left(1 - \frac{r_s r - r_Q^2}{\rho^2}\right)dt^2 - \left[r^2 + a^2 + a^2\sin^2\theta\left(\frac{r_g r - r_Q^2}{\rho^2}\right)\right]\sin^2\theta d\phi^2$$

$$+2\sin^2\theta\left(\frac{r_g r - r_Q^2}{\rho^2}\right)dtd\phi - \frac{\rho^2}{\Delta}dr^2 - \rho^2 d\theta^2,$$

$$\rho^2 = r^2 + a^2\cos^2\theta \qquad \Delta = r^2 - r_g r + a^2 + r_Q^2$$

Horizons are determined by

$$r_\pm = G_N(1+\alpha)M\left[1 \pm \sqrt{1 - \frac{a^2}{G_N^2(1+\alpha)^2M^2} - \frac{\alpha}{1+\alpha}}\right]$$

$$r_s = 2G_N(1+\alpha)M,\ a = J/M\ r_Q^2 = G_N^2\alpha(1+\alpha)M^2$$

Black Hole Shadows (Silhouettes) (T. Johannsen et al. arXiv:1512.02640 [astro-ph.GA])

We shall take it as given that our modified gravity–Schwarzschild and modified gravity–Kerr black holes are characterized by only the two parameters mass M and angular momentum J. They are stationary and asymptotically flat solutions and they satisfy the "no-hair" theorem. An interesting consequence of these properties of the solution is that the shadow outline created by the black hole is determined by M and $a = J/M$ and the relative position of an asymptotic observer.

The black hole casts a shadow in front of an illuminated background in the asymptotically flat region and the shadow is determined by a set of closed photon orbits. A photon moving on a circular orbit with radius r in our modified gravity–Kerr spacetime with nonzero a and M has the apparent position in the (x,y) reference frame of a distant observer located in the angle of latitude θ

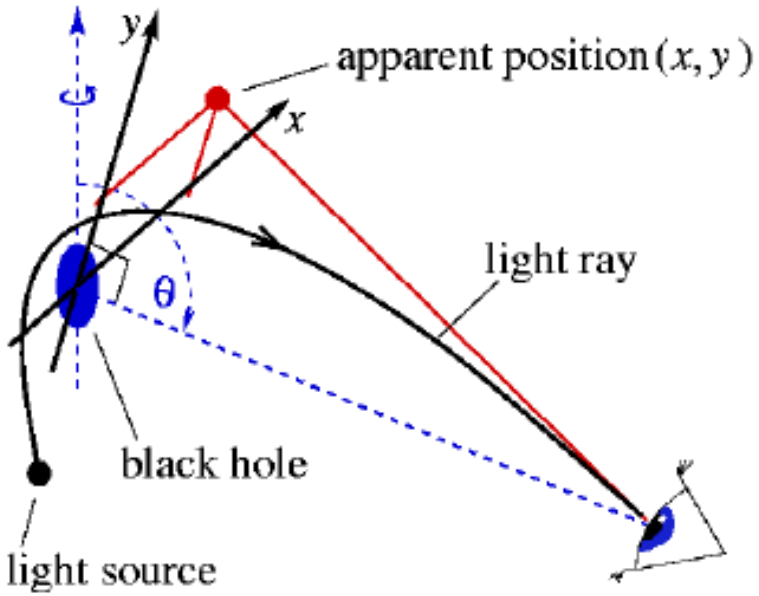

Figure 1: The apparent position of a light ray with respect to the observer's projection plane in the x,y coordinates containing the center of the spacetime: x denotes the apparent distance from the rotation axis, and y the projection of the rotation axis itself (dashed line). The angle θ denotes the angle of latitude, reaching from the north pole at $\theta = 0$ to the south pole at $\theta = \pi$ (image by de Vries).

The shadow radius for the Schwarzschild-MOG black hole is

$$r_{\rm shad} = \frac{\left[3(1+\alpha) \pm \sqrt{(9+\alpha)(1+\alpha)}\right]^2}{\left\{4\left[(1+\alpha) \pm \sqrt{(9+\alpha)(1+\alpha)}\right]^2 - 16(1+\alpha)\right\}^{1/2}} G_N M$$

The shadow radius can be approximated by

$$r_{\rm shad} \sim (2.59 + 2\alpha) r_s$$

The angular radius is given by $R = (5.19 + 4\alpha) r_g$ /D where D=8.3 kpc and $r_g = G_N M/c^2$. For α =0 and M = 4.23X 10^6 M_{SUN} we get

$$R = 26\,\mu as$$

For α = 1 we get

$$R = 46\,\mu \rm as$$

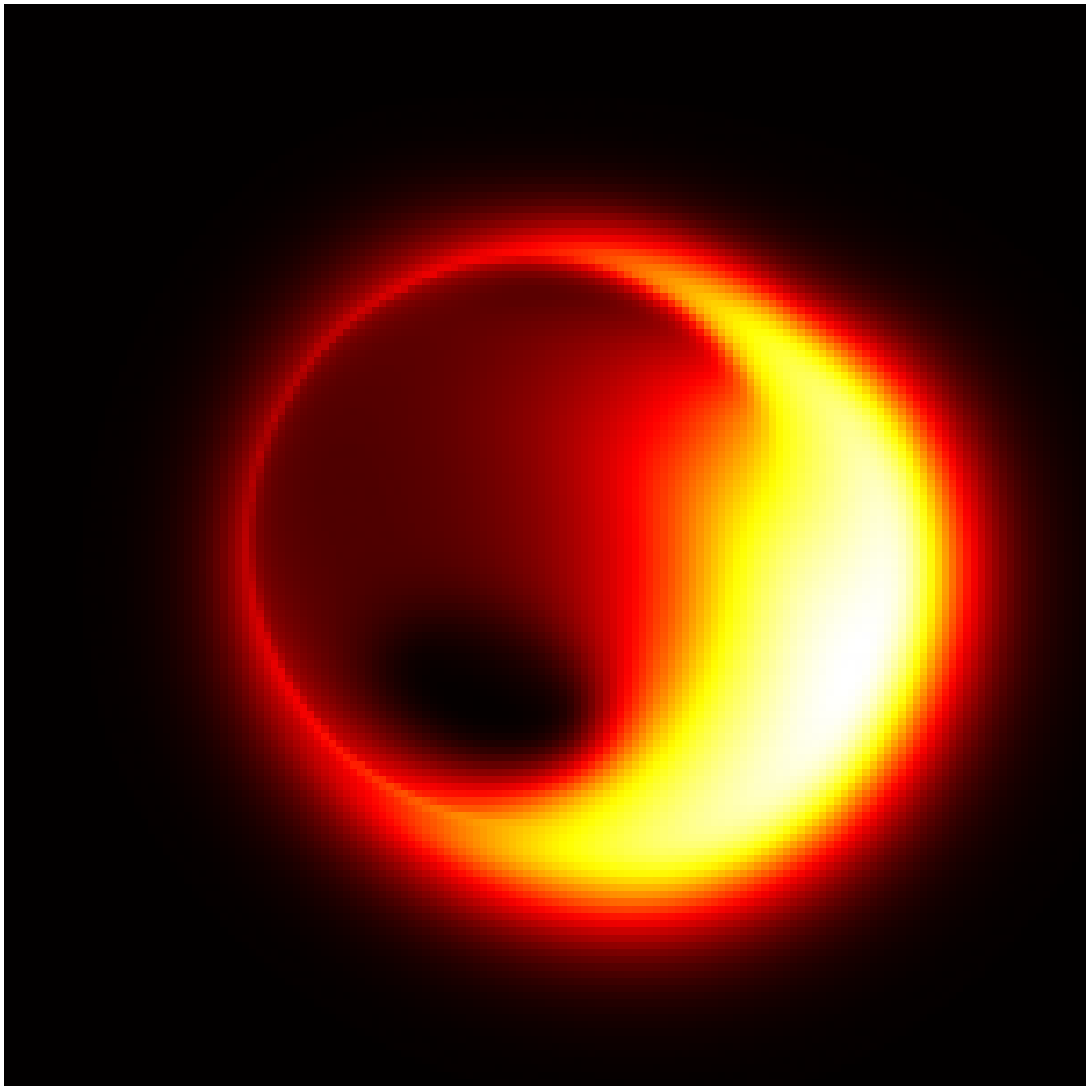

Computer-generated model of the Sagittarius A* black hole shadow. Image courtesy Avery Broderick at the Perimeter Institute for Theoretical Physics and the University of Waterloo

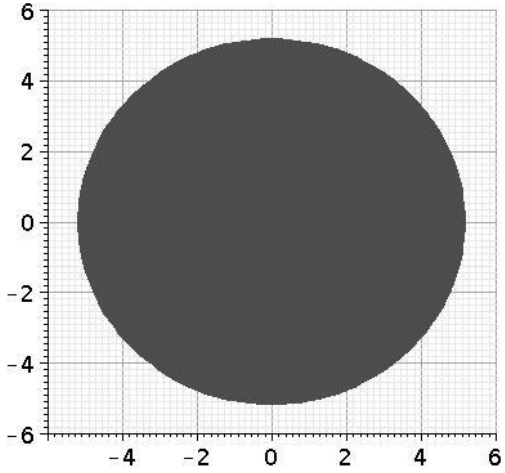

Schwarzschild BH a=0

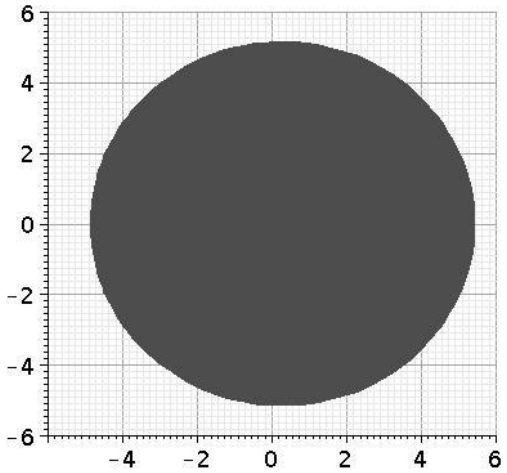

Kerr BH with a=0.16

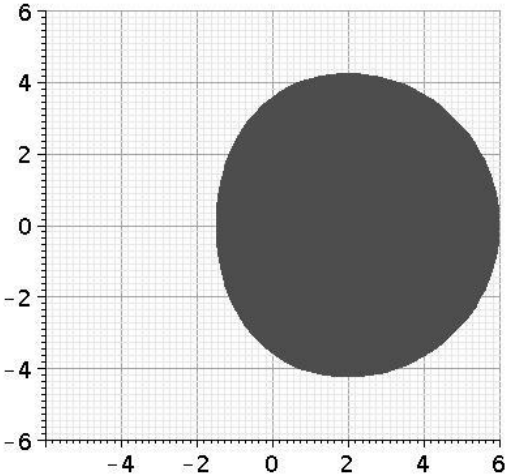

Kerr BH with a=0.95

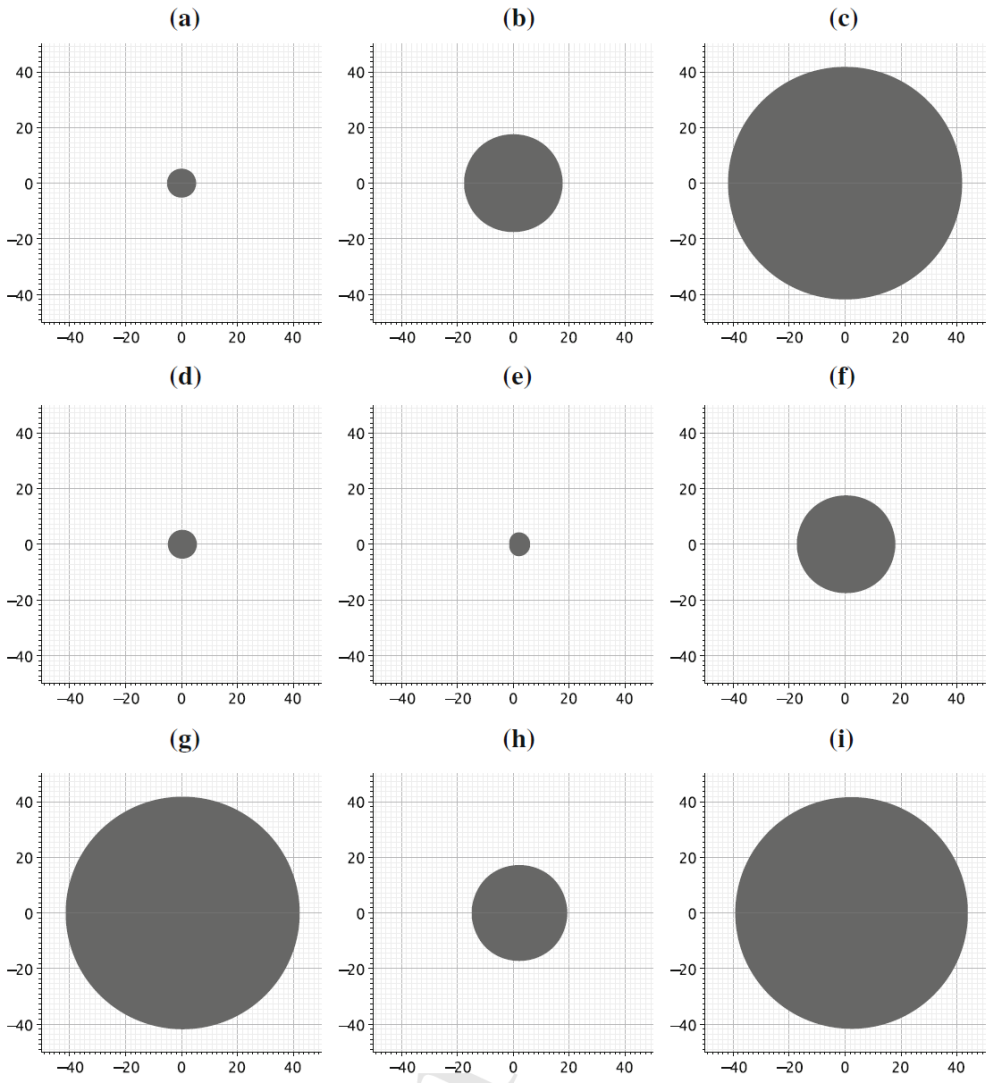
(a)
(b)
(c)
(d)
(e)
(f)
(g)
(h)
(i)
40
20
0
−20
−40
−40
−20
0
20
40

Black hole shadows for $G_N = 1$ and $M = 1$. $\theta = 63^0$, $0 \leq a \leq 0.95$, $0 \leq \alpha \leq 9$.

For $\alpha = 9$ the shadow radius obtained is $r_{\text{shad}} = 22.68 r_s$. The effect of the M^2 contribution in the modified gravity–Kerr shadow is to decrease the distortion of the circular shadow for $a \neq 0$ in the Kerr black hole shadow.

The Event Horizon Telescope observations should be able to determine the size and shape of the black hole shadow to 5 to 10 % accuracy, provided that the effect of the accretion disk surrounding the black hole can be determined. Successful observations can distinguish between strong gravity MOG black holes and GR back holes.

Orbit of S2/SO-2 Star in Sagittarius

Strong gravity field prediction for star S2/SO-2 orbiting black hole Sgr*.

semimajor axis = 5.5 light days

eccentricity = 0.881 ± 0.007

period = 15.56 ± 0.35 yr

Black Hole mass = $4.3 \times 10^6 M_{SUN}$

Periastron advance:

$\Delta\phi = (6\pi G_N M_{BH})/a(1-e^2) = 0.18^0/5$ yr

MOG predicts the same periastron advance as GR. The same holds true for the perihelion advance of Mercury: $\Delta\phi =$ 43 "/ century.

Experimental Data that can be fitted by MOG:

1. Planck and WMAP cosmic microwave background (CMB) data:

   Structure growth (stars and galaxies). ✓

   Angular acoustical power spectrum. ✓

   Matter power spectrum. ✓

   Accelerated expansion of the universe. ✓

2. Galaxy rotation curves. Galactic cluster dynamics. ✓
3. Bullet Cluster 1E0657-558 and Abell 520 “train wreck “ cluster collision. ✓
4. Gravitational lensing. ✓
5. Binary pulsar timing (PSR 1913+16). ✓
6. Solar system experiments. ✓
7. Strong gravity: Event Horizon Telescope and black holes. ?

Conclusions

- The modified gravity (MOG) theory can solve the problem of dark matter in early universe cosmology and late-time large scale structure galaxy and galaxy cluster dynamics. It provides a fully covariant gravitational action principle and field equations.
- The action principle contains, in addition to the metric Einstein-Hilbert action, a varying Newtonian constant G, a repulsive gravitational field ϕ_μ and an effective mass-range scalar field μ.
- The theory predicts structure growth, the expansion of the universe and the angular acoustical power spectrum in the CMB data. Galaxy and cluster dynamics are explained without detectable dark matter in the late-time universe. The predicted matter power spectrum can distinguish between MOG and ΛCDM. Galaxies do not possess a dark matter halo.
- Before recombination and before the formation of the first stars and galaxies, the gravitational strength vector field ϕ_μ is a cold dark matter ultralight particle γ'. After this epoch, the mass decreases to $m_\phi = 2.6 \times 10^{-28}$ eV, modified gravity takes over and enhanced gravity explains the galaxy and galaxy cluster dynamics in the late-time universe without dark matter.

- The singular Schwarzschild-MOG and Kerr-MOG black holes have no naked singularity solutions for non-zero values of the parameter α. The sizes and shapes of the MOG black holes grow for increasing values of α.

- The VLBI and EHT astronomical observations with small enough micro arc - second resolution can distinguish between the Schwarzschild-MOG, Kerr-MOG black holes and their GR counterparts, testing GR for strong gravitational fields.

- We have interpreted the dark energy using the cosmological constant Λ. Another possible model is to include a new dark massive photon field θ_μ in the MOG action with a field :

$$C_{\mu\nu} = \partial_\mu \theta_\nu - \partial_\nu \theta_\mu$$

This can mimic the cosmological constant $\Lambda \sim m_\theta^2$ with $m_\theta \sim 10^{-34}$ eV and agree with the standard ΛCDM cosmological model data: (S. Kouwn, P. Oh and C-G Park, arXiv:1512.00541 [gr-qc].)

END